LARGE-ORDER ASYMPTOTICS FOR MULTIPLE-POLE SOLITONS OF THE FOCUSING NONLINEAR SCHRÖDINGER EQUATION

DENIZ BILMAN AND ROBERT BUCKINGHAM

ABSTRACT. We analyze the large-n behavior of soliton solutions of the integrable focusing nonlinear Schrödinger equation with associated spectral data consisting of a single pair of conjugate poles of order $2n$. Starting from the zero background, we generate multiple-pole solitons by n-fold application of Darboux transformations. The resulting functions are encoded in a Riemann-Hilbert problem using the robust inverse-scattering transform method recently introduced by Bilman and Miller. For moderate values of n we solve the Riemann-Hilbert problem exactly. With appropriate scaling, the resulting plots of exact solutions reveal semiclassical-type behavior, including regions with high-frequency modulated waves and quiescent regions. We compute the boundary of the quiescent regions exactly and use the nonlinear steepest-descent method to prove the asymptotic limit of the solitons is zero in these regions. Finally, we study the behavior of the solitons in a scaled neighborhood of the central peak with amplitude proportional to n. We prove that in a local scaling the solitons converge to functions satisfying the second member of the Painlevé-III hierarchy in the sense of Sakka. This function is a generalization of a function recently identified by Suleimanov in the context of geometric optics and by Bilman, Ling, and Miller in the context of rogue wave solutions to the focusing nonlinear Schrödinger equation.

1. INTRODUCTION

The one-dimensional focusing cubic nonlinear Schrödinger equation

$$(1.1) \qquad i\psi_t + \frac{1}{2}\psi_{xx} + |\psi|^2\psi = 0, \quad x, t \in \mathbb{R}$$

is a standard model for the evolution of quasi-monochromatic waves in weakly nonlinear dispersive media [5] with applications including fluid dynamics [36] and nonlinear optics [12]. Solutions of (1.1) are well known to exhibit highly structured multiscale coherent wave patterns that may be viewed as the focusing counterpart to dispersive shock waves occuring in systems with hyperbolic modulation equations such as the defocusing nonlinear Schrödinger and Korteweg-de Vries equations [14]. A standard mechanism for the generation of rapid oscillations of $|\psi(x,t)|$ from smooth Cauchy data is the dispersive regularization of a so-called gradient catastrophe [6]. These phenomena have been extensively studied using the semiclassically scaled problem $i\epsilon\psi_t + \frac{\epsilon}{2}\psi_{xx} + |\psi|^2\psi = 0$ with ϵ-independent Cauchy data $\psi_0(x, 0)$. As $\epsilon \to 0$, the initial condition can be better approximated by reflectionless initial data consisting of $\mathcal{O}(\epsilon^{-1})$ solitons. These so-called semiclassical soliton ensembles can be computed explicitly for moderately small values of ϵ, and studied asymptotically via Riemann-Hilbert techniques in the limit $\epsilon \to 0$ [17, 20]. Solutions asymptotically display rapid oscillations of period $\mathcal{O}(\epsilon)$ in fixed (ϵ-independent) regions of the space-time plane.

The nonlinear Schrödinger equation (1.1) is completely integrable [37], and each initial condition with sufficient smoothness and decay is associated to scattering data consisting of poles and connection coefficients (encoding solitons) and a reflection coefficient (encoding radiation). The scattering data for a semiclassical soliton ensemble consists of $\mathcal{O}(\epsilon^{-1})$ *simple* poles (and associated connection coefficients, but the reflection coefficient is zero). On the other hand, it has been known since the original work of Zakharov and Shabat [37] that (1.1) has soliton solutions with spectral

---

data consisting of *higher-order* poles. We refer to a reflectionless solution of (1.1) with scattering data consisting of a pair of poles of order m as an mth-*order pole soliton* or, more generally, a *multiple-pole soliton*. In light of the rich mathematical structure displayed by solutions with scattering data consisting of a large number of simple poles, along with the fact that multiple-pole solitons can be generated by the coalescence of simple poles, it is natural to study the asymptotic behavior of mth-order pole solitons as $m \to \infty$. We show that multiple-pole solitons provide an alternate mechanism for generating behavior qualitatively similar to dispersive shock waves (see Figures 1–6).

Previous studies of muliple-pole soliton solutions of (1.1) have primarily focused on algebraic as opposed to asymptotic aspects [2, 16, 21, 30]. Olmedilla [23] and Schiebold [27] studied the long-time asymptotic behavior (while keeping the pole order fixed). Solitons associated to higher-order poles have also been studied for the modified Korteweg-de Vries equation [35], the sine-Gordon equation [3, 25, 32], the Caudrey-Dodd-Gibbon-Sawada-Kotera equation [15], the Kadomtsev-Petviashvili I equation [1, 33], the N-wave system [28], the complex short-pulse equation [19], and the coupled Sasa-Satsuma system [18]. Vinh [34] has recently studied analogues of higher-order solitons for nonintegrable generalized Korteweg-de Vries equations.

The recently introduced robust inverse-scattering transform [8] (see §2.1 for more details) provides the tools necessary to analyze the large-order behavior of multiple-pole solitons. Bilman, Ling, and Miller [7] used the robust inverse-scattering transform to study the large-order asymptotic behavior of multiple-pole soliton solutions of

$$(1.2) \qquad i\psi_t + \frac{1}{2}\psi_{xx} + (|\psi|^2 - 1)\psi = 0, \quad x, t \in \mathbb{R}$$

with non-decaying initial conditions (i.e. the nonlinear Schrödinger equation expressed in a rotating frame). Here we adapt the robust inverse-scattering transform to analyze multiple-pole soliton solutions of (1.1) generated by repeated Darboux transformations. Specifically, we fix a Darboux transformation that takes a given solution $\psi_0(x, t)$ to (1.1) and generates a new solution $\widetilde{\psi}_0(x, t)$ with the same Beals-Coifman scattering data except for the addition of double poles at points ξ and ξ^*. If the Beals-Coifman scattering data for $\psi_0(x, t)$ already has poles of order m at ξ and ξ^*, then the Beals-Coifman scattering data for $\widetilde{\psi}_0(x, t)$ will have poles of order $m + 2$ at these points. We start with the trivial initial condition $\psi^{[0]}(x, t) \equiv 0$ and repeatedly apply the same Darboux transformation n times to obtain a solution $\psi^{[2n]}(x, t)$ with order $2n$ poles at ξ and ξ^*.

As one might expect, the global behavior (the *far field*) is markedly different for the multiple-pole soliton solutions of (1.1) studied here and the multiple-pole soliton solutions of (1.2) studied in [7]. Nevertheless, the multiple-pole soliton solutions of (1.1) and (1.2) both have a peak of amplitude proportional to the pole order m. In [7], it was shown for (1.2) that the local behavior in a scaled neighborhood of this peak (the *near field*) is given by a certain Painlevé function. We show that for (1.1) the near-field behavior is described by a new family of Painlevé solutions that agree with the Painlevé function in [7] for special parameter values. We now summarize our results.

1.1. **Far-field results.** Fix a pole location $\xi \in \mathbb{C}^+$, a vector of connection coefficients $\mathbf{c} \equiv (c_1, c_2) \in (\mathbb{C}^*)^2$, and a non-negative integer n. Define $D_0 \subset \mathbb{C}$ to be a circular disk centered at the origin containing ξ in its interior. Let $\mathbf{M}^{[n]}(\lambda; x, t; \mathbf{c}) \equiv \mathbf{M}^{[n]}(\lambda; x, t)$ be the unique solution of the following Riemann-Hilbert problem (for uniqueness see the argument in, for example, [8, Theorem 2.4]).

Riemann-Hilbert Problem 1. *Let $(x, t) \in \mathbb{R}^2$ be arbitrary parameters, and let $n \in \mathbb{Z}_{\geq 0}$. Find the unique 2×2 matrix-valued function $\mathbf{M}^{[n]}(\lambda; x, t)$ with the following properties:*

> ***Analyticity:*** $\mathbf{M}^{[n]}(\lambda; x, t)$ *is analytic for $\lambda \in \mathbb{C} \setminus \partial D_0$, and it takes continuous boundary values from the interior and exterior of ∂D_0.*

Jump condition: *The boundary values on the jump contour ∂D_0 (oriented clockwise) are related as*

$$(1.3) \qquad \mathbf{M}_+^{[n]}(\lambda; x, t) = \mathbf{M}_-^{[n]}(\lambda; x, t) e^{-i(\lambda x + \lambda^2 t)\sigma_3} \mathbf{S} \left(\frac{\lambda - \xi}{\lambda - \xi^*} \right)^{n\sigma_3} \mathbf{S}^{-1} e^{i(\lambda x + \lambda^2 t)\sigma_3}, \quad \lambda \in \partial D_0,$$

where

$$(1.4) \qquad \mathbf{S} := \frac{1}{|\mathbf{c}|} \begin{pmatrix} c_1 & -c_2^* \\ c_2 & c_1^* \end{pmatrix}.$$

Normalization: $\mathbf{M}^{[n]}(\lambda; x, t) \to \mathbb{I}$ *as $\lambda \to \infty$.*

The $2n^{\text{th}}$-order pole solitons we study are defined by

$$(1.5) \qquad \psi^{[2n]}(x, t; \mathbf{c}) \equiv \psi^{[2n]}(x, t) := 2i \lim_{\lambda \to \infty} \lambda [\mathbf{M}^{[n]}(\lambda; x, t; \mathbf{c})]_{12}$$

(see Remark 1 in §2.3 for the explanation of why the pole order is necessarily even). Introduce the scaled space and time variables χ and τ by

$$(1.6) \qquad \chi := \frac{x}{n}, \quad \tau := \frac{t}{n}.$$

As illustrated in Figures 1 and 4, as $n \to \infty$ the $\chi\tau$-plane is partitioned into well-defined regions in which the leading-order behavior of $\psi^{[2n]}(n\chi, n\tau)$ is different. Figure 1 illustrates this convergence for $\xi = i$ and $\mathbf{c} = (1, 1)$.
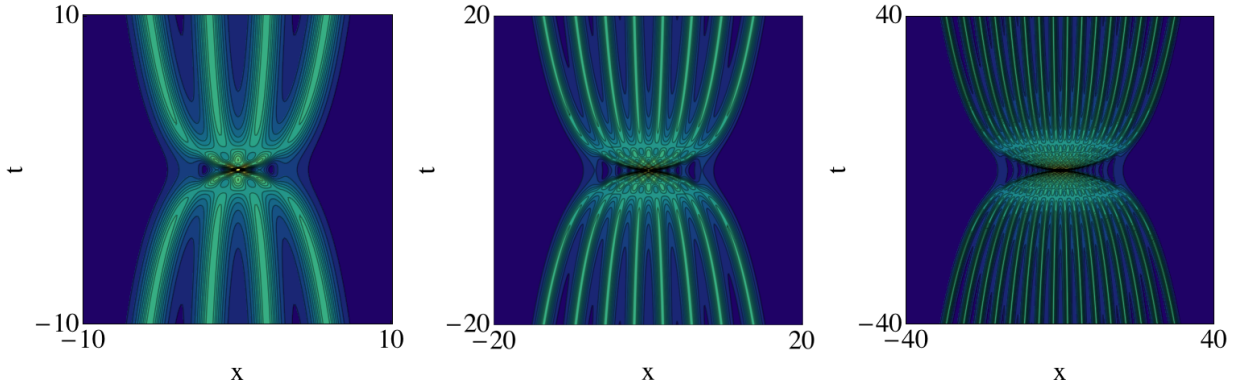

FIGURE 1. Plots of $|\psi^{[2n]}(x, t; (1, 1))|$ for $-5n \leq t \leq 5n$ and $-5n \leq x \leq 5n$ (i.e. $-5 \leq \tau \leq 5$ and $-5 \leq \chi \leq 5$), where $\psi^{[2n]}(x, t; (1, 1))$ is a multiple-pole soliton solution of the nonlinear Schrödinger equation (1.1). In each plot $c_1 = c_2 = 1$ and $\xi = i$. *Left: $n = 2$, Center: $n = 4$. Right: $n = 8$.*

Figures 2 and 3 show time slices of $|\psi^{[2n]}(n\chi, n\tau)|$ at $\tau = \frac{3}{8}$ and $\tau = 5$, respectively. Although it is beyond the scope of this paper, these plots suggest there are at least three different nonzero leading-order behaviors.
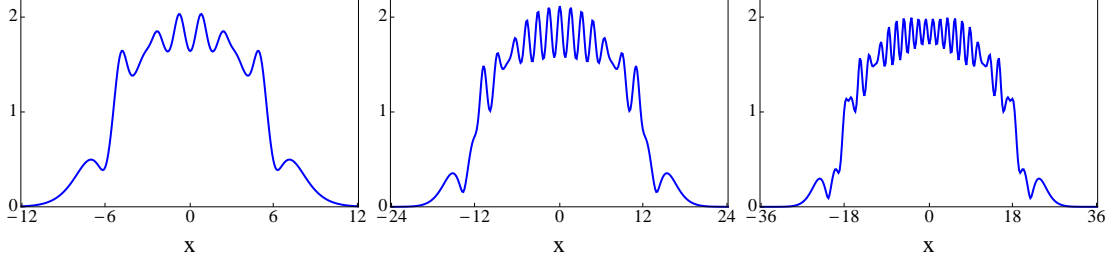
FIGURE 2. Plots of $|\psi^{[2n]}(x, \frac{3}{8}n; (1,1))|$ for $t = \frac{3}{8}n$ and $-3n \leq x \leq 3n$ (i.e. $\tau = \frac{3}{8}$ and $-3 \leq \chi \leq 3$), where $\psi^{[2n]}(x, t; (1,1))$ is a multiple-pole soliton solution of the nonlinear Schrödinger equation (1.1). In each plot $c_1 = c_2 = 1$ and $\xi = i$. *Left:* $n = 4$. *Center:* $n = 8$. *Right:* $n = 12$.
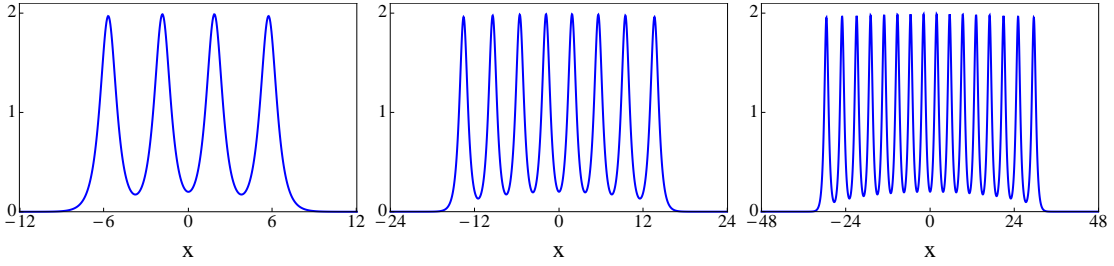

FIGURE 3. Plots of $|\psi^{[2n]}(x, 5n; (1,1))|$ for $t = 5n$ and $-6n \leq x \leq 6n$ (i.e. $\tau = 5$ and $-6 \leq \chi \leq 6$), where $\psi^{[2n]}(x, t; (1,1))$ is a multiple-pole soliton solution of the nonlinear Schrödinger equation (1.1). In each plot $c_1 = c_2 = 1$ and $\xi = i$. *Left:* $n = 2$. *Center:* $n = 4$. *Right:* $n = 8$.

In Figure 4 we illustrate the effect of changing **c** by plotting $\psi^{[2n]}(n\chi, n\tau)$ with **c** $= (1, 5)$. Much of the far-field structure remains the same. The solution appears to still be converging to zero at all (χ, τ) points at which the solution converged to zero with **c** $= (1, 1)$ (this is made precise in Theorem 1). Furthermore, if $|\tau|$ is sufficiently large, then the oscillatory structure appears unchanged. However, there are noticable qualitative differences for χ and τ near the origin.
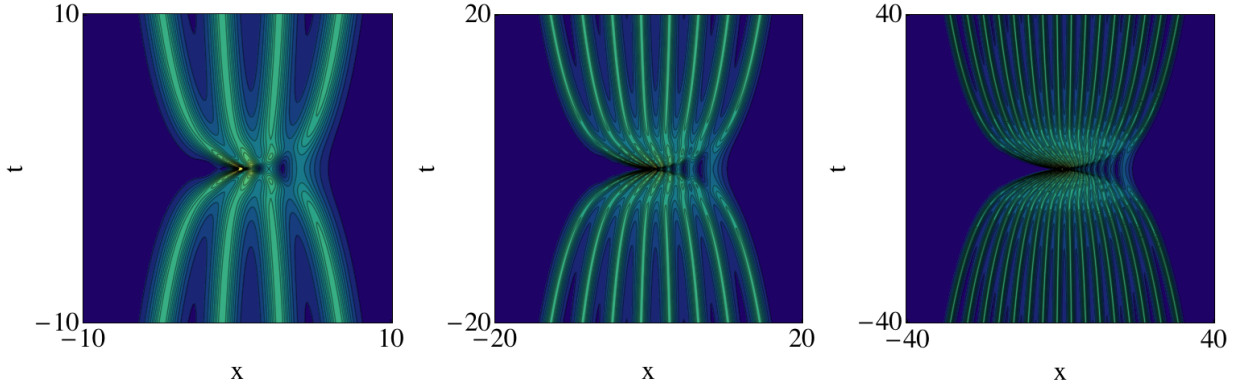

FIGURE 4. Plots of $|\psi^{[2n]}(x, t; (1,5))|$ for $-5n \leq t \leq 5n$ and $-5n \leq x \leq 5n$ (i.e. $-5 \leq \tau \leq 5$ and $-5 \leq \chi \leq 5$), where $\psi^{[2n]}(x, t; (1,5))$ is a multiple-pole soliton solution of the nonlinear Schrödinger equation (1.1). In each plot $c_1 = 1$, $c_2 = 5$, and $\xi = i$. *Left:* $n = 2$. *Center:* $n = 4$. *Right:* $n = 8$.

These differences are further illustrated in Figure 5, which shows a time slice at $\tau = \frac{3}{8}$ for $\mathbf{c} = (1, 5)$. We partially quantify these differences by studying the dependence on $\mathbf{c}$ in the near-field limit in Theorem 2.
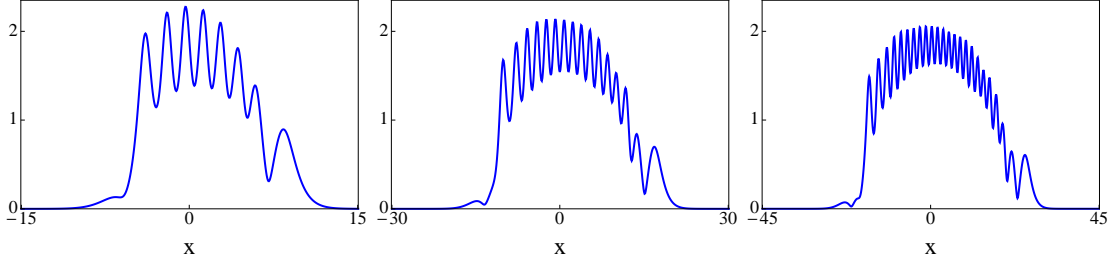

FIGURE 5. Plots of $|\psi^{[2n]}(x, \frac{3}{8}n; (1, 5))|$ for $t = \frac{3}{8}n$ and $-\frac{15}{4}n \le x \le \frac{15}{4}n$ (i.e. $\tau = \frac{3}{8}$ and $-\frac{15}{4} \le \chi \le \frac{15}{4}$), where $\psi^{[2n]}(x, t; (1, 5))$ is a multiple-pole soliton solution of the nonlinear Schrödinger equation (1.1). In each plot $c_1 = 1$, $c_2 = 5$, and $\xi = i$. *Left:* $n = 4$. *Center:* $n = 8$. *Right:* $n = 12$.

Our first result is Theorem 1, showing there is a specific region in the $\chi\tau$-plane in which $\psi^{[2n]}(n\chi, n\tau)$ decays exponentially fast to zero as $n \to \infty$. This region depends on ξ but is independent of $\mathbf{c}$. We provide an explicit (though transcendental) characterization of the boundary of the zero region.

We state our results for $\xi = i$, which is sufficient for general ξ by symmetry properties of (1.1) since there is only one conjugate pair of poles in the scattering data. Formulas for general ξ are provided in §3. The boundary curve consists of two different types of points. First, consider the locus of points $(\chi, \tau) \in \mathbb{R}^2$ satisfying

$$(1.7) \qquad 16\tau^4 + (8\chi^2 - 72\chi + 108)\tau^2 + (\chi^4 - 2\chi^3) = 0.$$

Part of this locus is a smooth arc with endpoints $\left(\frac{9}{4}, \pm\frac{3\sqrt{3}}{8}\right)$ and containing the point $(2, 0)$. Call this arc $\mathcal{L}_1$. This arc appears to separate the zero region from a region in which the leading-order behavior of $\psi^{[2n]}(n\chi, n\tau)$ is specified by a model Riemann-Hilbert problem with a single band (suggesting non-oscillatory behavior).

Next, given $\xi \in \mathbb{C}$, define the phase function

$$(1.8) \qquad \varphi(\lambda; \chi, \tau) := i(\lambda\chi + \lambda^2\tau) + \log\left(\frac{\lambda - \xi^*}{\lambda - \xi}\right).$$

The critical points of $\varphi(\lambda; \chi, \tau)$ are those values of λ satisfying

$$(1.9) \qquad 2\tau\lambda^3 + \chi\lambda^2 + 2\tau\lambda + (\chi - 2) = 0.$$

For $\tau = 0$ and $\chi > 2$, define

$$(1.10) \qquad \lambda_+(\chi, 0) := \left(\frac{2 - \chi}{\chi}\right)^{1/2}$$

so that $\Im(\lambda_+(\chi, 0)) > 0$. Note that if $\tau = 0$, then $\lambda_+(\chi, 0)$ satisfies (1.9). For $\tau \ge 0$, let $\lambda_+(\chi, \tau)$ be the solution of (1.9) that is the analytic continuation in τ of (1.10). We restrict this definition to (χ, τ) values that can be reached by a vertical path in the $\chi\tau$-plane starting at $(\chi, 0)$ along which no two solutions of (1.9) coincide. Then, the condition

$$(1.11) \qquad \Re(\varphi(\lambda_+(\chi, \tau), \chi, \tau)) = 0$$

defines a simple unbounded curve in the first quadrant of the $\chi\tau$-plane with one endpoint at $\left(\frac{9}{4}, \frac{3\sqrt{3}}{8}\right)$. Denote this curve by $\mathcal{L}_2^+$ and define $\mathcal{L}_2^- := \{(\chi, \tau) : (\chi, -\tau) \in \mathcal{L}_2^+\}$. The curves $\mathcal{L}_2^+$

and $\mathcal{L}_2^-$ appear to separate the zero region from regions in which the leading-order behavior of $\psi^{[2n]}(n\chi, n\tau)$ is specified by a model Riemann-Hilbert problem with two bands (suggesting oscillatory behavior). Let $\mathcal{Z}_+$ denote the unbounded region in the $\chi\tau$-plane containing the ray $\chi > 2$ and bounded by $\mathcal{L}_1 \cup \mathcal{L}_2^+ \cup \mathcal{L}_2^-$. Also define $\mathcal{Z}_- := \{(\chi, \tau) : (-\chi, -\tau) \in \mathcal{Z}_+\}$. Define the zero region $\mathcal{Z} := \mathcal{Z}_+ \cup \mathcal{Z}_-$.

Theorem 1. *If $(\chi, \tau) \in \mathcal{Z}$,*

$$(1.12) \qquad\qquad \psi^{[2n]}(n\chi, n\tau; \mathbf{c}) = \mathcal{O}(e^{-dn})$$

holds for some constant $d > 0$.

Theorem 1 holds for general $\xi \in \mathbb{C}^+$ with $\mathcal{Z}$ defined as in §3. The boundary curve is independent of both $\mathbf{c}$ and n, although it does depend on ξ (see §3 for the ξ-dependent formulas). Figure 6 illustrates the boundary curve for two choices of ξ.

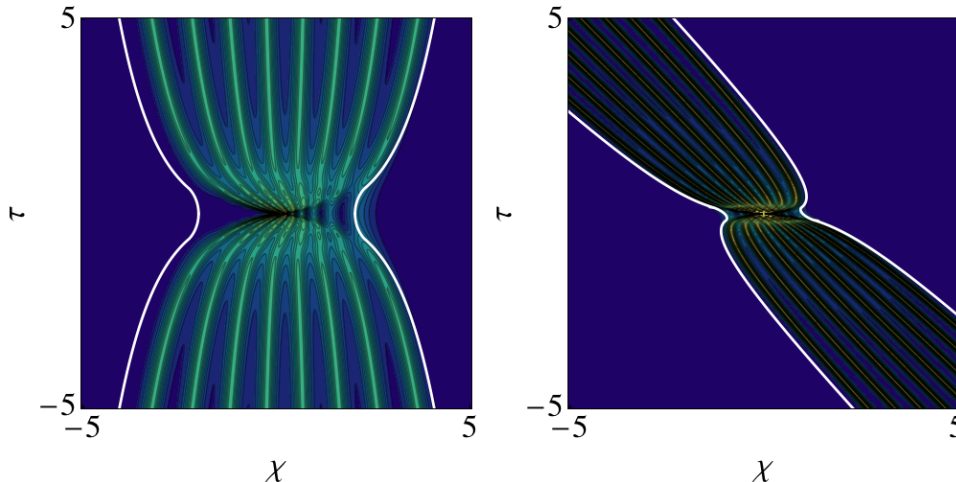
FIGURE 6. The boundary of the zero region for two choices of ξ. *Left:* Plot of $|\psi^{[2n]}(n\chi, n\tau; (1, 5))|$ with $c_1 = 1$, $c_2 = 5$, and $\xi = i$. *Right:* Plot of $|\psi^{[2n]}(n\chi, n\tau; (1, 1))|$ with $c_1 = 1$, $c_2 = 1$, and $\xi = \frac{1}{2} + 2i$. In both plots $n = 4$, $-5 \le \chi \le 5$, $-5 \le \tau \le 5$, and $\psi^{[2n]}(x, t; \mathbf{c})$ is a multiple-pole soliton solution of the nonlinear Schrödinger equation (1.1).

1.2. **Near-field results.** From plots such as Figure 7, it is evident that the qualitative behavior of $\psi^{[2n]}(x, t; \mathbf{c})$ near $(x, t) = (0, 0)$ is distinctly different from elsewhere in the space-time plane and is dominated by a single peak (with shape dependent on $\mathbf{c}$) with amplitude of $\mathcal{O}(n)$ for n large.
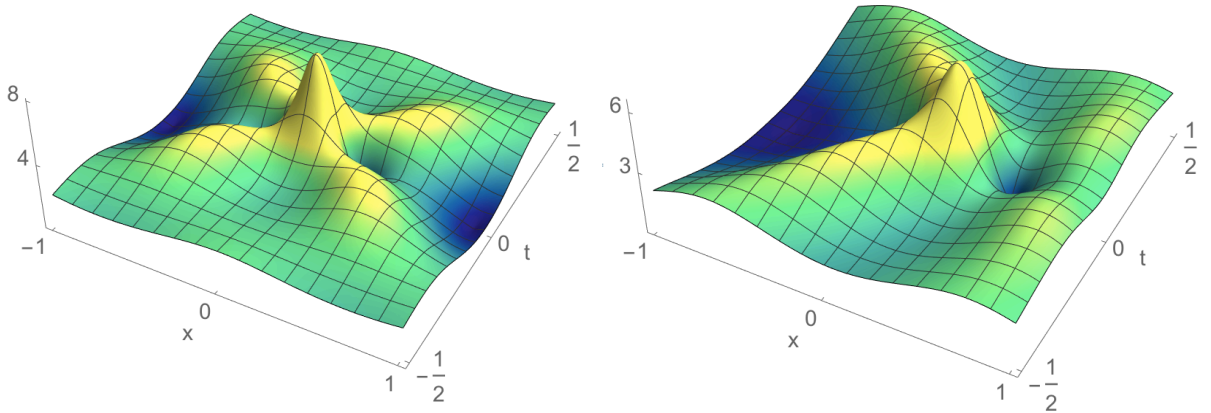
FIGURE 7. Plots of $|\psi^{[2]}(x,t;\mathbf{c})|$ illustrating the behavior near $(x,t) = (0,0)$, where $\psi^{[2]}(x,t;\mathbf{c})$ is a 2nd-order pole soliton solution of the nonlinear Schrödinger equation (1.1). *Left:* $\mathbf{c} = (1,1)$. *Right:* $\mathbf{c} = (1,5)$.

We study the behavior in this region by defining the rescaled variables

$$(1.13) \qquad\qquad X := nx, \quad T := n^2 t.$$

Our main result is that, in the large-n limit, the function $\frac{1}{n}\psi^{[2n]}(\frac{X}{n},\frac{T}{n^2};\mathbf{c})$ is well-approximated by a function $\Psi(X,T;\mathbf{c}) \equiv \Psi(X,T)$ that satisfies Painlevé-III hierarchy equations in the sense of Sakka [26]. The functions $\Psi(X,T;(1,1))$ and $\Psi(X,T;(1,-1))$ (with $\xi = i$) were first identified recently in two different but related contexts, self-focusing in nonlinear geometric optics [29] and rogue waves [7]. The work [7], which is more closely related to the current study, analyzes solutions of the focusing nonlinear Schrödinger equation (1.2) generated from repeated Darboux transformations applied to the constant solution $\psi(x,t) \equiv 1$. The resulting solutions, referred to in [7] as fundamental rogue waves, can be viewed as higher-order analogues of the Peregrine breather. The spectral data encoding the fundamental rogue waves includes a conjugate pair of singularities of fractional order (as opposed to a pair of poles of integer order in our situation). The far-field behavior is completely different behavior for the two problems (compare, say, Figure 1 above with Figure 2 in [7]), and it is only in an appropriate scaling near the origin that the functions $\Psi(X,T)$ emerge. This situation in which the local behavior of more than one solution is described by the same Painlevé transcendent or other special function is a hallmark of integrable wave equations.

Some of the main results concerning these functions in [7] are as follows:

(a′) Fundamental rogue-wave solutions of (1.2) near the origin are, after appropriate scaling, well approximated by certain functions $\Psi(X,T;(1,\pm1))$ that are solutions of (1.1).

(b′) For fixed T, the functions $\Psi(X,T;(1,\pm1))$ satisfy the second member of Sakka's Painlevé-III hierarchy [26] with certain parameters. These functions satisfy $\Psi(0,0;(1,\pm1)) = \pm4$, $\Psi(-X,T;(1,\pm1)) = \Psi(X,T;(1,\pm1))$, and $\Psi(X,-T;(1,\pm1)) = \Psi(X,T;(1,\pm1))^*$.

(c′) For $T = 0$, the functions $\Psi(X,0;(1,\pm1))$ generate certain solutions of the Painlevé-III equation.

In this work we prove analogues of (a′)–(c′) for the higher-order pole soliton solutions of (1.1). We start with a more general Darboux transformation than in [7, 8], allowing both general $\xi \in \mathbb{C}^+$ and general $\mathbf{c} \in (\mathbb{C}^*)^2$. The choice of ξ can effectively be scaled out and does not introduce new phenomena, so we will fix $\xi = i$. However, changing $\mathbf{c}$ amounts to changing the boundary conditions of $\Psi(X,T;\mathbf{c})$, leading to a new family of distinguished Painlevé solutions. We emphasize that $\Psi(X,T;\mathbf{c})$ depends only on the ratio c_1/c_2, so in effect it is a one-(complex)-parameter family of

solutions (see the discussion at the end of §2.2). We illustrate the convergence of $\frac{1}{n}\psi^{[2n]}(\frac{X}{n}, 0; \mathbf{c})$ to $\Psi(X, 0; \mathbf{c})$ for $\mathbf{c} = (1, 1)$ and $\mathbf{c} = (1, 5)$ in Figures 8 and 9, respectively. The plots of $\frac{1}{n}\psi^{[2n]}(\frac{X}{n}, 0; \mathbf{c})$ ($n = 2, 4, 8$) were generated by solving the associated Riemann-Hilbert problem recast as a linear system (see Appendix A). The functions $\Psi(X, 0; \mathbf{c})$ were computed using the methodology introduced in [31] and `RHPackage` [24] (see Appendix B). Note that the even X-symmetry enjoyed by $\Psi(X, 0; (1, \pm 1))$ is broken for general $\mathbf{c}$.
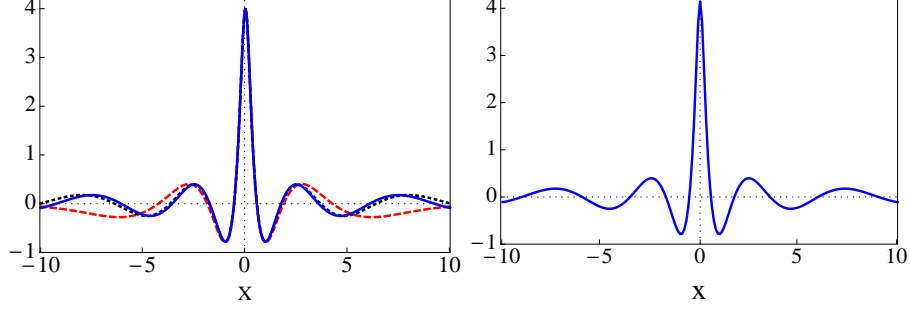

FIGURE 8. *Left:* Scaled multiple-pole soliton solutions $\frac{1}{n}\psi^{[2n]}(\frac{X}{n}, 0; (1, 1))$ of the nonlinear Schrödinger equation (1.1) for $T = 0$ and $-10 \leq X \leq 10$ (i.e. $t = 0$ and $-\frac{10}{n} \leq x \leq \frac{10}{n}$) for $n = 2$ (red and dashed), $n = 4$ (black and dotted), and $n = 8$ (blue and solid) with $\mathbf{c} = (1, 1)$. *Right:* The limiting function $\Psi(X, 0; (1, 1))$ with $\mathbf{c} = (1, 1)$.
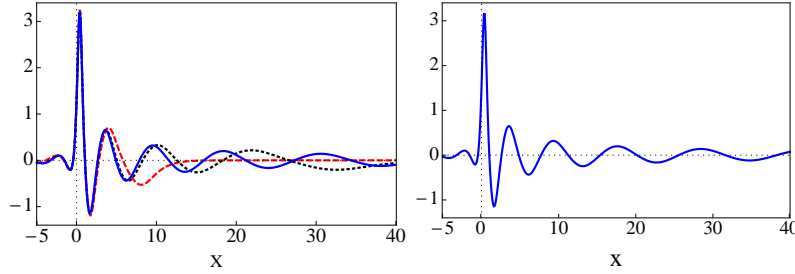
FIGURE 9. *Left:* Scaled multiple-pole soliton solutions $\frac{1}{n}\psi^{[2n]}(\frac{X}{n}, 0; (1, 5))$ of the nonlinear Schrödinger equation (1.1) for $T = 0$ and $-5 \leq X \leq 40$ (i.e. $t = 0$ and $-\frac{5}{n} \leq x \leq \frac{40}{n}$) for $n = 2$ (red and dashed), $n = 4$ (black and dotted), and $n = 8$ (blue and solid) with $\mathbf{c} = (1, 5)$. *Right:* The limiting function $\Psi(X, 0; (1, 5))$ with $\mathbf{c} = (1, 5)$.

We now state our near-field results.

Theorem 2. *Fix* $\mathbf{c} \equiv (c_1, c_2) \in (\mathbb{C}^*)^2$ *and set* $\xi = i$. *Then the following hold.*

(a) *There is an n-independent function $\Psi(X, T; \mathbf{c})$ such that, as $n \to \infty$,*

$$(1.14) \qquad \frac{1}{n}\psi^{[2n]}\left(\frac{X}{n}, \frac{T}{n^2}; \mathbf{c}\right) = \Psi(X, T; \mathbf{c}) + \mathcal{O}\left(\frac{1}{n}\right)$$

uniformly for compact subsets of the XT-plane. The function $\Psi(X, T; \mathbf{c})$ is a solution of (1.1) in the variables X and T, i.e.

$$(1.15) \qquad i\Psi_T + \frac{1}{2}\Psi_{XX} + |\Psi|^2\Psi = 0, \quad X, T \in \mathbb{R}.$$

(b) *For fixed $T \in \mathbb{R}$, the function $\Psi(X, T; \mathbf{c})$ satisfies the fourth-order ordinary differential equation*

$$
\begin{aligned}
(1.16) \quad & X\Psi\Psi_{XXX} + 3\Psi\Psi_{XX} - X\Psi_X\Psi_{XX} - 2(\Psi_X)^2 + 4\Psi^3\Psi^* + 2X\Psi^2\Psi^*\Psi_X + 2X\Psi^3\Psi_X^* \\
& + iT(\Psi\Psi_{XXXX} - \Psi_X\Psi_{XXX} + 6\Psi^2\Psi_X\Psi_X^* + 6\Psi^2\Psi^*\Psi_{XX}) = 0,
\end{aligned}
$$

which is the second member of Sakka's Painlevé-III hierarchy [26] with certain parameters. Also, $\Psi(X, T; \mathbf{c})$ satisfies the initial conditions

$$
(1.17) \qquad \Psi(0, 0; \mathbf{c}) = 8\frac{c_1 c_2^*}{|\mathbf{c}|^2}, \quad \Psi_X(0, 0; \mathbf{c}) = 32\frac{c_1 c_2^*}{|\mathbf{c}|^4}(c_2 c_2^* - c_1 c_1^*),
$$

as well as the symmetries

$$
(1.18) \qquad \Psi(-X, T; \mathbf{c}^*\sigma_1) = \Psi(X, T; \mathbf{c})
$$

and

$$
(1.19) \qquad \Psi(X, -T; \mathbf{c})^* = \Psi(X, T; \mathbf{c}) \text{ if } \mathbf{c} \in \mathbb{R}^2.
$$

In particular, if $\mathbf{c} \in \mathbb{R}^2$ then $\Psi(X, 0; \mathbf{c})$ is real-valued.

(c) *If $\mathbf{c} \in \mathbb{R}^2$, then*

$$
(1.20) \qquad u(s; \mathbf{c}) := \frac{2s^2\Psi(-\frac{1}{8}s^2, 0; \mathbf{c})}{(s^2\Psi(-\frac{1}{8}s^2, 0; \mathbf{c}))_s}
$$

satisfies the standard Painlevé-III equation

$$
(1.21) \qquad u_{ss} = \frac{1}{u}(u_s)^2 - \frac{1}{s}u_s + \frac{4\Theta_0 u^2 + 4(1 - \Theta_\infty)}{s} + 4u^3 - \frac{4}{u}
$$

with parameters $\Theta_\infty = \Theta_0 = 0$. The odd function $u(s; \mathbf{c})$ satisfies

$$
(1.22) \qquad u_s(0; \mathbf{c}) = 1, \quad u_{sss}(0; \mathbf{c}) = \frac{3}{|\mathbf{c}|^2}(c_2^2 - c_1^2).
$$

1.3. Outline and notation.

In §2 we define the Darboux transformation that generates $\psi^{[2n]}(x, t)$ from $\psi^{[2n-2]}(x, t)$ and use the robust inverse-scattering transform recently introduced by Bilman and Miller [8] to derive Riemann-Hilbert Problem 1 encoding $\psi^{[2n]}(x, t)$. In §3 we analyze this Riemann-Hilbert problem in the far-field scaling (1.6) and prove Theorem 1 concerning the zero region. In §4 we consider the near-field scaling (1.13) and prove Theorem 2 showing the local behavior near the origin is described by the solution $\Psi(X, T)$ of Sakka's Painlevé-III hierarchy. In Appendix A we show how the basic Riemann-Hilbert problem can be reformulated as a linear system, a fact used to plot $\psi^{[2n]}(x, t)$ in Figures 1–9. In Appendix B we describe how RHPackage is used to compute $\Psi(X, T)$ for Figures 8 and 9.

Notation. We define

$$
(1.23) \qquad \mathbb{I} := \begin{pmatrix} 1 & 0 \\ 0 & 1 \end{pmatrix}, \quad \sigma_1 := \begin{pmatrix} 0 & 1 \\ 1 & 0 \end{pmatrix}, \quad \sigma_2 := \begin{pmatrix} 0 & -i \\ i & 0 \end{pmatrix}, \quad \sigma_3 := \begin{pmatrix} 1 & 0 \\ 0 & -1 \end{pmatrix}.
$$

With the exception of the identity matrix and the Pauli matrices, we denote 2×2 matrices by bold upper-case letters and 2-vectors by bold lower-case letters. If $\mathbf{M}$ is a matrix, the jk-entry of $\mathbf{M}$ is denoted by $[\mathbf{M}]_{jk}$. The complex conjugate of a number a is denoted a^*, while the conjugate-transpose of a vector $\mathbf{v}$ is denoted $\mathbf{v}^\dagger$. By $\mathbb{C}^*$ we mean $\mathbb{C}\backslash\{0\}$, while by $\mathbb{C}^+$ we mean $\{z \in \mathbb{C} : \Im(z) > 0\}$. The boundary of a domain $D \subset \mathbb{C}$ is denoted ∂D. When we write $f(x; s)$ we mean that f is a function of x with parametric dependence on s, and we may suppress the explicit dependence on parameters for brevity.

2. The Darboux transformation and initial Riemann-Hilbert problem

2.1. **Summary of the robust inverse scattering transform.** We begin with a brief overview of the robust inverse-scattering transform introduced recently in [8] and how it differs from the standard inverse-scattering transform. The basis for any inverse-scattering trasform for (1.1) is the Lax pair [37]

$$(2.1) \quad \begin{aligned} \frac{\partial \mathbf{u}}{\partial x}(\lambda; x, t) &= \begin{bmatrix} -i\lambda & \psi(x,t) \\ -\psi(x,t) & i\lambda \end{bmatrix} \mathbf{u}(\lambda; x, t), \\ \frac{\partial \mathbf{u}}{\partial t}(\lambda; x, t) &= \begin{bmatrix} -i\lambda^2 + \frac{i}{2}|\psi(x,t)|^2 & \lambda\psi(x,t) + \frac{i}{2}\psi_x(x,t) \\ -\lambda\psi(x,t)^* + \frac{i}{2}\psi_x(x,t)^* & i\lambda^2 - \frac{i}{2}|\psi(x,t)|^2 \end{bmatrix} \mathbf{u}(\lambda; x, t). \end{aligned}$$

The standard inverse-scattering transform [4] begins by defining the Jost matrices $\mathbf{J}^\pm(\lambda; x, t)$ to be the unique fundamental matrix of simultaneous solutions to (2.1) satisfying the boundary conditions $\mathbf{J}^\pm(\lambda; x, t)e^{i\lambda x\sigma_3} = \mathbb{I} + o(1)$, $x \to \pm\infty$. The Jost functions also satisfy the scattering relation

$$(2.2) \quad \mathbf{J}^+(\lambda; x, t) = \mathbf{J}^-(\lambda; x, t) \begin{bmatrix} a(\lambda^*)^* & b(\lambda^*; t)^* \\ -b(\lambda; t) & a(\lambda) \end{bmatrix}.$$

If we denote the first and second columns of $\mathbf{J}^\pm$ by $\mathbf{j}^{\pm,1}$ and $\mathbf{j}^{\pm,2}$, respectively, then we can define the Beals-Coifman simultaneous solution to (2.1) as

$$(2.3) \quad \mathbf{U}^{\mathrm{BC}}(\lambda; x, t) := \begin{cases} \left[\frac{1}{a(\lambda)}\mathbf{j}^{-,1}(\lambda; x, t)e^{-i\lambda^2 t}, \quad \mathbf{j}^{+,2}(\lambda; x, t)e^{i\lambda^2 t}\right], & \lambda \in \mathbb{C}^+, \\ \left[\mathbf{j}^{+,1}(\lambda; x, t)e^{-i\lambda^2 t}, \quad \frac{1}{a(\lambda^*)^*}\mathbf{j}^{-,2}(\lambda; x, t)e^{i\lambda^2 t}\right], & \lambda \in \mathbb{C}^-. \end{cases}$$

Then the function

$$(2.4) \quad \mathbf{M}^{\mathrm{BC}}(\lambda; x, t) := \mathbf{U}^{\mathrm{BC}}(\lambda; x, t)e^{i(\lambda x + \lambda^2 t)\sigma_3}$$

satisfies the normalization condition

$$(2.5) \quad \lim_{\lambda \to \infty} \mathbf{M}^{\mathrm{BC}}(\lambda; x, t) = \mathbb{I},$$

the Schwarz-symmetry condition

$$(2.6) \quad \mathbf{M}^{\mathrm{BC}}(\lambda; x, t) = \sigma_2 \mathbf{M}^{\mathrm{BC}}(\lambda^*; x, t)^* \sigma_2, \quad \lambda \in \mathbb{C}\backslash\mathbb{R},$$

and the jump condition

$$(2.7) \quad \mathbf{M}_+^{\mathrm{BC}}(\lambda; x, t) = \mathbf{M}_-^{\mathrm{BC}}(\lambda; x, t) \begin{bmatrix} 1 + |R(\lambda)|^2 & R(\lambda)^* e^{-2i(\lambda x + \lambda^2 t)} \\ R(\lambda)e^{2i(\lambda x + \lambda^2 t)} & 1 \end{bmatrix}, \quad \lambda \in \mathbb{R},$$

where $R(\lambda) := b(\lambda; t)/a(\lambda)$. These properties allow $\mathbf{M}^{\mathrm{BC}}(\lambda; x, t)$ to be obtained as the solution of a Riemann-Hilbert problem.

The function $\mathbf{M}^{\mathrm{BC}}(\lambda; x, t)$ has nice properties as $\lambda \to \infty$ (i.e. (2.5)). However, for general λ $\mathbf{M}^{\mathrm{BC}}(\lambda; x, t)$ is only sectionally *meromorphic*, with poles arising from zeros of $a(\lambda)$ corresponding to solitons. In general, these poles can be handled in the Riemann-Hilbert formalism either by solving the problem exactly (as we do in Appendix A) or by interpolation (see, for instance, [17]). There are technical issues with unique solvability of the Riemann-Hilbert problem with spectral singularities, i.e. points in the continuous spectrum for which $\mathbf{M}^{\mathrm{BC}}(\lambda; x, t)$ fails to have a boundary value [8, §1.1.2]. These spectral singulares, which arise in particular in the case of Peregrine breathers, can be handled by a limiting procedure. The robust inverse-scattering transform bypasses the limiting procedure and leads directly to a sectionally analytic Riemann-Hilbert problem, even for solutions whose scattering data under the standard inverse-scattering transform consist of spectral singularities of high order (i.e higher-order Peregrine breathers) [7]. While we are not concerned with spectral singularities in the current work, we take advantage of the robust inverse-scattering transform's ability to handle higher-order poles.

The key observation of the robust inverse-scattering transform is that different fundamental solutions of (2.1) have desirable properties in different sections of the λ-plane. The Beals-Coifman solution $\mathbf{U}^{\mathrm{BC}}(\lambda; x, t)$ is well-behaved for $|\lambda|$ sufficiently large. On the other hand, there are other solutions that are bounded in the regions where $\mathbf{U}^{\mathrm{BC}}(\lambda; x, t)$ has poles. The following key proposition is proved in [8, Proposition 2.1] for (1.2); nevertheless the proof goes through verbatim for (1.1).

Proposition 1. *Suppose $\psi(x, t)$ is a bounded classical solution of (1.1) defined for (x, t) in a simply connected domain $\Omega \subset \mathbb{R}^2$ containing $(0, 0)$. Then, for each $\lambda \in \mathbb{C}$, there exists a unique simultaneous fundamental solution matrix $\mathbf{U}^{\mathrm{in}}(\lambda; x, t)$, $(x, t) \in \Omega$, of the Lax pair equations (2.1) together with the initial condition $\mathbf{U}^{\mathrm{in}}(\lambda; 0, 0) = \mathbb{I}$. Furthermore, $\mathbf{U}^{\mathrm{in}}(\lambda; x, t)$ is an entire function of λ for each $(x, t) \in \Omega$, $\det \mathbf{U}^{\mathrm{in}}(\lambda; x, t) \equiv 1$, and $\mathbf{U}^{\mathrm{in}}(\lambda; x, t) = \sigma_2 \mathbf{U}^{\mathrm{in}}(\lambda^*; x, t)^* \sigma_2$.*

Now define $D_0 \subset \mathbb{C}$ to be an open disk centered at the origin of sufficiently large radius to contain all the singularities of $\mathbf{U}^{\mathrm{BC}}(\lambda; x, t)$. Set

$$(2.8) \qquad \mathbf{U}(\lambda; x, t) := \begin{cases} \mathbf{U}^{\mathrm{in}}(\lambda; x, t), & \lambda \in D_0, \\ \mathbf{U}^{\mathrm{BC}}(\lambda; x, t), & \text{otherwise} \end{cases}$$

and define $\Sigma_L := (-\infty, -r)$, $\Sigma_R := (r, \infty)$, $\Sigma_+ := \partial D_0 \cap \mathbb{C}^+$, $\Sigma_- := \partial D_0 \cap \mathbb{C}^-$ (Σ_L and Σ_R are oriented left-to-right while Σ_+ and Σ_- are oriented clockwise). Then the function

$$(2.9) \qquad \mathbf{M}(\lambda; x, t) := \mathbf{U}(\lambda; x, t) e^{i(\lambda x + \lambda^2 t)\sigma_3}, \quad \lambda \in \mathbb{C} \backslash \mathbb{R}, \quad (x, t) \in \mathbb{R}^2$$

is analytic for $\lambda \notin \Sigma_L \cup \Sigma_R \cup \Sigma_+ \cup \Sigma_-$, satisfies the jump (2.7) on $\Sigma_L \cup \Sigma_R$, and has the jump

$$(2.10) \qquad \mathbf{M}_+(\lambda; x, t) = \begin{cases} \mathbf{M}_-(\lambda; x, t) \left[\frac{1}{a(\lambda)} \mathbf{j}^{-,1}(\lambda; 0, 0), \quad \mathbf{j}^{+,2}(\lambda; 0, 0) \right], & \lambda \in \Sigma^+, \\ \mathbf{M}_-(\lambda; x, t) \left[\mathbf{j}^{+,1}(\lambda; 0, 0), \quad \frac{1}{a(\lambda^*)^*} \mathbf{j}^{-,2}(\lambda; 0, 0) \right], & \lambda \in \Sigma^- \end{cases}$$

on the remaining contours. Thus, in addition to having identity asymptotics at infinity (see (2.5)), $\mathbf{M}(\lambda; x, t)$ satisfies a jump condition in a form amenable to analysis via the nonlinear steepest-descent method of Deift and Zhou [13]. Once $\mathbf{M}(\lambda; x, t)$ is known, the solution to (1.1) can be found by

$$(2.11) \qquad \psi(x, t) = 2i \lim_{\lambda \to \infty} \lambda [\mathbf{M}(\lambda; x, t)]_{12}.$$

2.2. **Definition of the Darboux transformation.** We now define the specific Darboux transformations we will use and show how to formulate them in terms of the robust inverse-scattering transform. The basic idea of a Darboux transformation is to take a solution of (1.1) and find the solution having the same Beals-Coifman scattering data with the exception of one or more additional poles (see [22] for further background).

We begin by defining certain Darboux transformations depending on an eigenvalue $\xi = \alpha + i\beta \in \mathbb{C}^+$ and a row vector of connection coefficients $\mathbf{d} := (d_1, d_2) \in \mathbb{C}^2$. The Darboux transformations we study will be derived from these by taking a certain limit of $\mathbf{d}$. Given the matrix $\mathbf{U}(\lambda; x, t)$ defined in (2.8) and associated to a solution $\psi(x, t)$ of (1.1), we introduce

$$(2.12) \qquad \dot{\mathbf{U}}(\lambda; x, t) := \left(\mathbb{I} + \frac{\mathbf{R}(x, t)}{\lambda - \xi} \right) \mathbf{U}(\lambda; x, t)$$

for a to-be-determined matrix $\mathbf{R}(x, t)$. The transformation (2.12) is constructed so that $\dot{\mathbf{U}}(\lambda; x, t)$ has the same jump conditions and normalization as $\lambda \to \infty$ as $\mathbf{U}(\lambda; x, t)$. If we further assume that $\mathbf{R}(x, t)^2 = \mathbf{0}$, then we also have $\det \dot{\mathbf{U}}(\lambda; x, t) = 1$. The remaining freedom in determining $\mathbf{R}(x, t)$ can be used to ensure

$$(2.13) \qquad \operatorname*{Res}_{\lambda = \xi} \dot{\mathbf{U}}(\lambda; x, t) = \lim_{\lambda \to \xi} \dot{\mathbf{U}}(\lambda; x, t) \begin{bmatrix} d_1 \\ d_2 \end{bmatrix} \begin{bmatrix} id_2 & -id_1 \end{bmatrix} = \lim_{\lambda \to \xi} \dot{\mathbf{U}}(\lambda; x, t) \begin{bmatrix} id_1 d_2 & -id_1^2 \\ id_2^2 & -id_1 d_2 \end{bmatrix}.$$

This condition completely specifies $\mathbf{R}(x,t)$ (see [8, §3.1] for complete details) as

$$(2.14) \qquad \mathbf{R}(x,t) = \frac{\mathbf{U}(\xi;x,t)\mathbf{d}^\mathsf{T}\mathbf{d}\mathbf{U}(\xi;x,t)^\mathsf{T}\sigma_2}{1 - \mathbf{d}\mathbf{U}(\xi;x,t)^\mathsf{T}\sigma_2\mathbf{U}'(\xi;x,t)\mathbf{d}^\mathsf{T}}.$$

At this point we would like to define $\dot{\mathbf{M}}(\lambda;x,t) := \dot{\mathbf{U}}(\lambda;x,t)e^{i(\lambda x + \lambda^2 t)\sigma_3}$ and set up the associated Riemann-Hilbert problem. The problem is that $\dot{\mathbf{M}}(\lambda;x,t)$ is not Schwarz-symmetric (i.e. does not satisfy an analogue of (2.6)), and thus cannot generate a solution of (1.1). This can be remedied by first performing a Darboux transformation $\mathbf{U}(\lambda;x,t) \to \dot{\mathbf{U}}(\lambda;x,t)$ with data $(\xi,\mathbf{d})$, and then performing a second Darboux transformation $\dot{\mathbf{U}}(\lambda;x,t) \to \ddot{\mathbf{U}}(\lambda;x,t)$ with data $(\xi^*,(\mathbf{d}\sigma_2)^*)$. We now write the composition of these two Darboux transformations explicitly (the interested reader can find full details of the straightforward calculation in [8, §3.2]). Define

$$(2.15) \qquad \begin{aligned} \mathbf{s}_\mathrm{f}(x,t) &:= \mathbf{U}(\xi;x,t)\mathbf{d}^\mathsf{T}, \quad N_\mathrm{f}(x,t) := \mathbf{s}_\mathrm{f}(x,t)^\dagger\mathbf{s}_\mathrm{f}(x,t), \\ w_\mathrm{f}(x,t) &:= \mathbf{d}\mathbf{U}(\xi;x,t)^\mathsf{T}\sigma_2\mathbf{U}'(\xi;x,t)\mathbf{d}^\mathsf{T} \end{aligned}$$

(here the subscript f stands for "finite") and use these to define

$$(2.16) \qquad \begin{aligned} \mathbf{Y}_\mathrm{f}(x,t) :=& \frac{4\beta^2(1 - w_\mathrm{f}(x,t)^*)}{4\beta^2|1 - w_\mathrm{f}(x,t)|^2 + N_\mathrm{f}(x,t)^2}\mathbf{s}_\mathrm{f}(x,t)\mathbf{s}_\mathrm{f}(x,t)^\mathsf{T}\sigma_2 \\ &+ \frac{2i\beta N_\mathrm{f}(x,t)}{4\beta^2|1 - w_\mathrm{f}(x,t)|^2 + N_\mathrm{f}(x,t)^2}\sigma_2\mathbf{s}_\mathrm{f}(x,t)^*\mathbf{s}_\mathrm{f}(x,t)^\mathsf{T}\sigma_2, \\ \mathbf{Z}_\mathrm{f}(x,t) :=& \sigma_2\mathbf{Y}_\mathrm{f}(x,t)^*\sigma_2. \end{aligned}$$

Then

$$(2.17) \qquad \ddot{\mathbf{U}}(\lambda;x,t) = \mathbf{G}_\mathrm{f}(\lambda;x,t)\mathbf{U}(\lambda;x,t),$$

where

$$(2.18) \qquad \mathbf{G}_\mathrm{f}(\lambda;x,t) := \mathbb{I} + \frac{\mathbf{Y}_\mathrm{f}(x,t)}{\lambda - \xi} + \frac{\mathbf{Z}_\mathrm{f}(x,t)}{\lambda - \xi^*}.$$

If we apply the general Darboux transformation defined by (2.17) to the trivial background solution $\psi(x,t) \equiv 0$, the resulting position of the generated solution can be shifted by replacing (d_1,d_2) with $(\epsilon^{-1}d_1,\epsilon^{-1}d_2)$ for some fixed constant $\epsilon \in \mathbb{C}^*$. We choose to fix two complex constants c_1 and c_2 and study the Darboux transformation with connection data $(\epsilon^{-1}c_1,\epsilon^{-1}c_2)$ in the limit $\epsilon \to 0$. This will have in particular the effect of ensuring $\psi(x,t;(1,\pm1))$ achieves its maximum value at the origin $(x,t) = (0,0)$. The formulas used to construct the Darboux transformation all have well-defined limits as $\epsilon \to 0$ that are given explicitly in (2.21)–(2.23) below. We note that those formulas are unchanged if both c_1 and c_2 are multiplied by the same nonzero complex number. Because of this, we can think of $\mathbf{c}$ as an element of the complex projective space $\mathbb{CP}^1$. This means that, although we write both c_1 and c_2, there is actually only *one* complex degree of freedom in the Darboux transformation. Furthermore, if either $c_1 = 0$ or $c_2 = 0$ then the limiting Darboux transformation defined by (2.21)–(2.23) is trivial (i.e. takes the input solution $\psi(x,t)$ to itself). Thus we restrict ourselves to $\mathbf{c} \in (\mathbb{C}^*)^2$.

2.3. **Iteration of the Darboux transformation.** If we apply the Darboux transformation with data $\{\xi,\mathbf{c}\}$ to the trivial solution

$$(2.19) \qquad \psi^{[0]}(x,t) \equiv 0$$

then we obtain a second-order pole soliton $\psi^{[2]}(x,t;\mathbf{c})$. In the same way, applying the Darboux transformation n times in succession (using the robust inverse-scattering transformation each time to sweep the spectral poles to ∂D_0) will generate a $2n^\mathrm{th}$-order pole soliton $\psi^{[2n]}(x,t;\mathbf{c})$. In principal

there is no need to fix the data $\{\xi, \mathbf{c}\}$ between iterations, although we will do so in order to obtain a well-defined limit as $n \to \infty$. We now explain the construction in detail.

Fix $\xi \in \mathbb{C}^+$ and $\mathbf{c} = (c_1, c_2) \in (\mathbb{C}^*)^2$. We begin with the background eigenvector matrix

$$(2.20) \qquad \mathbf{U}^{[0]}(\lambda; x, t) := e^{-i(\lambda x + \lambda^2 t)\sigma_3}$$

corresponding to the trivial solution (2.19). Let D_0 be a circular disc centered at the origin that is large enough to contain ξ. Suppose that $\mathbf{U}^{[n]}(\lambda; x, t)$ is known and is analytic for $\lambda \notin \partial D_0$. Set

$$(2.21) \qquad \begin{aligned} \mathbf{s}^{[n]}(x, t) &:= \mathbf{U}^{[n]}(\xi; x, t)\mathbf{c}^{\mathsf{T}}, \quad N^{[n]}(x, t) := \mathbf{s}^{[n]}(x, t)^{\dagger}\mathbf{s}^{[n]}(x, t), \\ w^{[n]}(x, t) &:= \mathbf{c}\mathbf{U}^{[n]}(\xi; x, t)^{\mathsf{T}}\sigma_2 \mathbf{U}^{[n]\prime}(\xi; x, t)\mathbf{c}^{\mathsf{T}}. \end{aligned}$$

Then define

$$(2.22) \qquad \mathbf{G}^{[n]}(\lambda; x, t) := \mathbb{I} + \frac{\mathbf{Y}^{[n]}(x, t)}{\lambda - \xi} + \frac{\mathbf{Z}^{[n]}(x, t)}{\lambda - \xi^*},$$

wherein

$$(2.23) \qquad \begin{aligned} \mathbf{Y}^{[n]}(x, t) :=& \frac{-4\beta^2 w^{[n]}(x, t)^*}{4\beta^2 |w^{[n]}(x, t)|^2 + N^{[n]}(x, t)^2}\mathbf{s}^{[n]}(x, t)\mathbf{s}^{[n]}(x, t)^{\mathsf{T}}\sigma_2 \\ &+ \frac{2i\beta N^{[n]}(x, t)}{4\beta^2 |w^{[n]}(x, t)|^2 + N^{[n]}(x, t)^2}\sigma_2 \mathbf{s}^{[n]}(x, t)^*\mathbf{s}^{[n]}(x, t)^{\mathsf{T}}\sigma_2, \\ \mathbf{Z}^{[n]}(x, t) :=& \sigma_2 \mathbf{Y}^{[n]}(x, t)^*\sigma_2. \end{aligned}$$

Define

$$(2.24) \qquad \ddot{\mathbf{U}}^{[n+1]}(\lambda; x, t) := \mathbf{G}^{[n]}(\lambda; x, t)\mathbf{U}^{[n]}(\lambda; x, t).$$

Now $\ddot{\mathbf{U}}^{[n+1]}(\lambda; x, t)$ has simple poles at ξ and ξ^*. We apply the idea of the robust inverse-scattering transform and sweep the poles to ∂D_0 by defining $\ddot{\mathbf{U}}^{[n,\mathrm{in}]}(\lambda; x, t) := \ddot{\mathbf{U}}^{[n]}(\lambda; x, t)\mathbf{G}^{[n]}(\lambda; 0, 0)^{-1}$ for $\lambda \in D_0$. Then the matrix

$$(2.25) \qquad \mathbf{U}^{[n+1]}(\lambda; x, t) := \begin{cases} \mathbf{G}^{[n]}(\lambda; x, t)\mathbf{U}^{[n]}(\lambda; x, t), & \lambda \notin D_0, \\ \mathbf{G}^{[n]}(\lambda; x, t)\mathbf{U}^{[n]}(\lambda; x, t)\mathbf{G}^{[n]}(\lambda; 0, 0)^{-1}, & \lambda \in D_0 \end{cases}$$

is analytic for $\lambda \notin \partial D_0$. In terms of the matrix $\mathbf{Y}^{[n]}$, the solution $\psi^{[2n+2]}(x, t)$ to (1.1) is obtained from the solution $\psi^{[2n]}(x, t)$ by

$$(2.26) \qquad \psi^{[2n+2]}(x, t) = \psi^{[2n]}(x, t) + 2i([\mathbf{Y}^{[n]}(x, t)]_{12} - [\mathbf{Y}^{[n]}(x, t)^*]_{21}).$$

For reference we perform the first Darboux transformation explicitly. Writing $\mathbf{s}^{[0]} = \left(s_1^{[0]}, s_2^{[0]}\right)^{\mathsf{T}}$, from (2.26), (2.19), and (2.23) we see

$$(2.27) \qquad \psi^{[2]} = \frac{-8\beta^2 w^{[0]*}(s_1^{[0]})^2 + 8\beta^2 w^{[0]}(s_2^{[0]*})^2 + 8\beta N^{[0]}s_1^{[0]}s_2^{[0]*}}{4\beta^2 |w^{[0]}|^2 + (N^{[0]})^2}.$$

We also have (writing $\xi = \alpha + i\beta$)

$$(2.28) \qquad \begin{aligned} s_1^{[0]}(x, t) &= c_1 e^{-i(\xi x + \xi^2 t)}, \quad s_2^{[0]}(x, t) = c_2 e^{i(\xi x + \xi^2 t)}, \\ w^{[0]}(x, t) &= 2c_1 c_2(x + 2\xi t), \quad N^{[0]}(x, t) = |c_1|^2 e^{2\beta x + 4\alpha\beta t} + |c_2|^2 e^{-2\beta x - 4\alpha\beta t}. \end{aligned}$$

Combining the previous two equations gives an explicit formula for $\psi^{[2]}(x, t)$ for any choice of $c_1, c_2 \in \mathbb{C}^*$ and $\xi \in \mathbb{C}^+$.

Remark 1. Looking at Figures 3 and 4, it appears that $\psi^{[2n]}(x,t)$ is a coalescence of $2n$ single-pole solitons (and this is indeed the case). Yet the observant reader may have noticed that $\psi^{[2n]}(x,t)$ is generated from the trivial background by only n applications of the Darboux transformation (2.25), each of which only involves a single pole. How do the n extra poles arise? To understand this, note that the right (i.e normalized as $x \to +\infty$) Beals-Coifman matrix $\mathbf{U}^{\mathrm{BC}}(\lambda; x,t)$ associated to $\psi^{[2n]}(x,t)$ with poles of order $2n$ at $\lambda = \xi$ and $\lambda = \xi^*$ has the asymptotic behavior

(2.29)
$$\begin{cases} \displaystyle\lim_{x \to +\infty} \mathbf{U}^{\mathrm{BC}}(\lambda; x,t)e^{i(\lambda x + \lambda^2 t)\sigma_3} = \mathbb{I}, \\ \mathbf{U}^{\mathrm{BC}}(\lambda; x,t)e^{i(\lambda x + \lambda^2 t)\sigma_3} \text{ is bounded as } x \to -\infty, \end{cases} \qquad \lambda \notin D_0, \ \Im(\lambda) > 0.$$

However, the matrix $\mathbf{U}^{[2n]}(\lambda; x,t)$ has different asymptotics as $x \to +\infty$ for $\Im(\lambda) > 0$, and it is necessary to renormalize to obtain the associated Beals-Coifman matrix, which introduces the additional pole at each iteration.

Remark 2. If one wanted to study the sequence of odd-order pole solitons $\{\psi^{[2n+1]}(x,t)\}$, then one could start with the standard single-pole soliton $\psi^{[1]}(x,t)$ and apply the Darboux transformation (2.25) n times. We anticipate that the large-n behavior of the odd sequence is the same as that of the even sequence, and so we restrict our attention to $\psi^{[2n]}(x,t)$.

2.4. **The Riemann-Hilbert problem.** Given $\mathbf{U}^{[n]}(\lambda; x,t)$, we define

(2.30)
$$\mathbf{M}^{[n]}(\lambda; x,t) := \mathbf{U}^{[n]}(\lambda; x,t)e^{i(\lambda x + \lambda^2 t)\sigma_3}.$$

We now pose the Riemann-Hilbert problem satisfied by $\mathbf{M}^{[n]}(\lambda; x,t)$. Orient ∂D_0 clockwise. From (2.25) and (2.30), we see the jump for $\mathbf{M}^{[n]}(\lambda; x,t)$ is

(2.31)
$$\mathbf{M}^{[n]}_+(\lambda; x,t) = \mathbf{M}^{[n]}_-(\lambda; x,t)\mathbf{V}^{[n]}_{\mathbf{M}}(\lambda; x,t), \quad \lambda \in \partial D_0,$$

where

(2.32)
$$\mathbf{V}^{[n]}_{\mathbf{M}}(\lambda; x,t) = e^{-i(\lambda x + \lambda^2 t)\sigma_3}\mathbf{G}^{[n-1]}(\lambda; 0,0) \cdots \mathbf{G}^{[1]}(\lambda; 0,0)\mathbf{G}^{[0]}(\lambda; 0,0)e^{i(\lambda x + \lambda^2 t)\sigma_3}.$$

Explicit evaluation of $\mathbf{Y}^{[n]}(0,0)$ shows it is actually independent of n, and so $\mathbf{G}^{[n]}(\lambda; 0,0) = \mathbf{G}^{[0]}(\lambda; 0,0)$ for all n. The reason for this is the point $(x,t) = (0,0)$ is the normalization point of $\mathbf{U}^{\mathrm{in}}(\lambda; x,t)$ in Proposition 1, and hence the values of the quantities (2.21) coincide at $(0,0)$ for each n. Thus

(2.33)
$$\mathbf{V}^{[n]}_{\mathbf{M}}(\lambda; x,t) := e^{-i(\lambda x + \lambda^2 t)\sigma_3}\mathbf{G}^{[0]}(\lambda; 0,0)^n e^{i(\lambda x + \lambda^2 t)\sigma_3}.$$

From (2.22) we have

(2.34)
$$\mathbf{G}^{[0]}(\lambda; 0,0) = \mathbb{I} + \frac{\mathbf{Y}^{[0]}(0,0)}{\lambda - \xi} + \frac{\mathbf{Z}^{[0]}(0,0)}{\lambda - \xi^*}.$$

By direct calculation we have

(2.35)
$$\mathbf{Y}^{[0]}(0,0) = \frac{2i\beta}{|\mathbf{c}|^2}\sigma_2(\mathbf{c}^*)^{\mathsf{T}}\mathbf{c}\sigma_2 = \frac{2i\beta}{|\mathbf{c}|^2}\begin{pmatrix} c_2 c_2^* & -c_1 c_2^* \\ -c_1^* c_2 & c_1 c_1^* \end{pmatrix}$$

and

(2.36)
$$\mathbf{Z}^{[0]}(0,0) = \sigma_2 \mathbf{Y}^{[0]}(0,0)^* \sigma_2 = \frac{-2i\beta}{|\mathbf{c}|^2}\begin{pmatrix} c_1 c_1^* & c_1 c_2^* \\ c_1^* c_2 & c_2 c_2^* \end{pmatrix}.$$

The eigenvalues of $\mathbf{G}^{[0]}(\lambda; 0,0)$ are $\frac{\lambda - \xi}{\lambda - \xi^*}$ and $\frac{\lambda - \xi^*}{\lambda - \xi}$. Recall the eigenvector matrix $\mathbf{S}$ defined by (1.4). We define a second eigenvector matrix by

(2.37)
$$\widetilde{\mathbf{S}} := \frac{1}{|\mathbf{c}|}\begin{pmatrix} c_2^* & c_1 \\ -c_1^* & c_2 \end{pmatrix}.$$

Then we have the following two useful representations of the jump matrix for $\mathbf{M}^{[n]}(\lambda; x, t)$:

(2.38)
$$\mathbf{V_M}^{[n]}(\lambda; x, t) = e^{-i(\lambda x + \lambda^2 t)\sigma_3} \mathbf{S} \begin{pmatrix} \left(\frac{\lambda-\xi}{\lambda-\xi^*}\right)^n & 0 \\ 0 & \left(\frac{\lambda-\xi^*}{\lambda-\xi}\right)^n \end{pmatrix} \mathbf{S}^{-1} e^{i(\lambda x + \lambda^2 t)\sigma_3}$$

$$= e^{-i(\lambda x + \lambda^2 t)\sigma_3} \widetilde{\mathbf{S}} \begin{pmatrix} \left(\frac{\lambda-\xi^*}{\lambda-\xi}\right)^n & 0 \\ 0 & \left(\frac{\lambda-\xi}{\lambda-\xi^*}\right)^n \end{pmatrix} \widetilde{\mathbf{S}}^{-1} e^{i(\lambda x + \lambda^2 t)\sigma_3}.$$

We therefore have the basic Riemann-Hilbert Problem 1 for $\mathbf{M}^{[n]}(\lambda; x, t)$. The $2n^{\text{th}}$-order pole soliton $\psi^{[2n]}(x, t; \mathbf{c})$ is obtained from $\mathbf{M}^{[n]}(\lambda; x, t)$ via (1.5).

3. ANALYSIS IN THE ZERO REGION

We now prove Theorem 1. Starting with $\mathbf{M}^{[n]}(\lambda; x, t)$, we perform a series of invertible transformations to analyze Riemann-Hilbert Problem 1 asymptotically. Recall $\chi := x/n$ and $\tau := t/n$ as introduced in (1.6). If $\chi > 0$, define

(3.1) $\mathbf{N}^{[n]}(\lambda; \chi, \tau) := \begin{cases} \mathbf{M}^{[n]}(\lambda; n\chi, n\tau) e^{-in(\lambda\chi + \lambda^2\tau)} \mathbf{S} e^{in(\lambda\chi + \lambda^2\tau)}, & \lambda \in D_0, \\ \mathbf{M}^{[n]}(\lambda; n\chi, n\tau) \left(\frac{\lambda-\xi^*}{\lambda-\xi}\right)^{n\sigma_3}, & \lambda \notin D_0 \end{cases}$ $(\chi > 0).$

If $\chi < 0$, define

(3.2) $\mathbf{N}^{[n]}(\lambda; \chi, \tau) := \begin{cases} \mathbf{M}^{[n]}(\lambda; n\chi, n\tau) e^{-in(\lambda\chi + \lambda^2\tau)} \widetilde{\mathbf{S}} e^{in(\lambda\chi + \lambda^2\tau)}, & \lambda \in D_0, \\ \mathbf{M}^{[n]}(\lambda; n\chi, n\tau) \left(\frac{\lambda-\xi}{\lambda-\xi^*}\right)^{n\sigma_3}, & \lambda \notin D_0 \end{cases}$ $(\chi < 0).$

The normalization for $\mathbf{N}^{[n]}(\lambda; \chi, \tau)$ as $\lambda \to \infty$ is unchanged from that of $\mathbf{M}^{[n]}(\lambda; \chi, \tau)$. Introducing the phase functions $\varphi(\lambda; \chi, \tau)$ by (1.8) and $\widetilde{\varphi}(\lambda; \chi, \tau)$ by

(3.3)
$$\widetilde{\varphi}(\lambda; \chi, \tau) := i(\lambda\chi + \lambda^2\tau) + \log\left(\frac{\lambda-\xi}{\lambda-\xi^*}\right),$$

the jump matrices for $\mathbf{N}^{[n]}(\lambda; \chi, \tau)$ can be written as

(3.4)
$$\mathbf{V_N}^{[n]}(\lambda; \chi, \tau) := \begin{cases} e^{-n\varphi(\lambda;\chi,\tau)\sigma_3} \mathbf{S}^{-1} e^{n\varphi(\lambda;x,t)\sigma_3}, & \chi > 0, \\ e^{-n\widetilde{\varphi}(\lambda;\chi,\tau)\sigma_3} \widetilde{\mathbf{S}}^{-1} e^{n\widetilde{\varphi}(\lambda;x,t)\sigma_3}, & \chi < 0 \end{cases}$$

for $\lambda \in \partial D_0$ (oriented clockwise). Note that $\varphi(\lambda; \chi, \tau)$ and $\widetilde{\varphi}(\lambda; \chi, \tau)$ are independent of $\mathbf{c}$.

Our immediate goal is to understand the topology of the level curves $\Re(\varphi(\lambda; \chi, \tau)) = 0$ in the complex λ-plane as χ and τ vary. Note that $\Re(\varphi(\lambda; \chi, \tau))$ is zero for all $\lambda \in \mathbb{R}$. Also, observe the critical points are those λ values satisfying

(3.5) $2\tau(\lambda - \alpha)^3 + (\chi + 2\alpha\tau)(\lambda - \alpha)^2 + 2\beta^2\tau(\lambda - \alpha) + (\beta^2\chi - 2\beta + 2\alpha\beta^2\tau) = 0.$

This cubic has real coefficients.

Assume first that $\tau = 0$. Then there are two critical points

(3.6)
$$\lambda_{\pm}(\chi, 0) = \alpha \pm \left(\frac{2\beta - \beta^2\chi}{\chi}\right)^{1/2}$$

(we write $(\cdot)^{1/2}$ for the principal branch of the square root). If $\chi = \frac{2}{\beta}$, then the two critical points coincide at α. If $\chi > \frac{2}{\beta}$, then $\lambda_{\pm}(\chi, 0)$ are complex conjugates. As we will see shortly, the ray $\{(\chi, \tau) : \chi > \frac{2}{\beta}, \tau = 0\}$ is in the zero region, so we assume $\chi \geq \frac{2}{\beta}$. As $\lambda \to \infty$, $i\lambda\chi$ is the dominant term in $\varphi(\lambda; \chi, 0)$, so $\Re(\varphi(\lambda; \chi, 0)) < 0$ for $\Im(\lambda) > 0$ and $\Re(\varphi(\lambda; \chi, 0)) > 0$ for $\Im(\lambda) < 0$ if $|\lambda|$ is sufficiently large. Looking at the logarithm term, $\Re(\varphi(\lambda; \chi, 0)) > 0$ for $|\lambda - \xi|$ sufficiently small, and $\Re(\varphi(\lambda; \chi, 0)) < 0$ for $|\lambda - \xi^*|$ sufficiently small. Therefore there must be a level line curve

$\Re(\varphi(\lambda; \chi, 0)) = 0$ completely enclosing $\lambda = \xi$ (and another around $\lambda = \xi^*$). Since $\Re(\varphi(\lambda; \chi, 0))$ is harmonic (and not constant) away from ξ and ξ^*, there can be at most one closed loop of the zero level lines in the upper half-plane and at most one in the lower half-plane. Therefore, the zero level curves must be exactly the real axis along with two simple loops enclosing ξ and ξ^* that intersect the real axis at a single (shared) point if $\chi = \frac{2}{\beta}$ (as shown in the left panel in Figure 10) or that are entirely in their respective half-planes if $\chi > \frac{2}{\beta}$ (as shown in the center panel in Figure 10). By explicit calculation, we check that $\lambda_\pm(\chi, 0)$ lie outside the two closed loops if $\chi > \frac{2}{\beta}$.

Now fix $\chi > \frac{2}{\beta}$. For $\tau > 0$ sufficiently small, $\varphi(\lambda; \chi, \tau)$ has three distinct critical points. Two of these form a complex conjugate pair with real part approximately α. We define $\lambda_\pm(\chi, \tau)$ to be the analytic continuation (in τ) of $\lambda_\pm(\chi, 0)$. This analytic continuation is well defined if τ is sufficiently small such that $\lambda_+(\chi, S) \neq \lambda_-(\chi, S)$ for $0 \le S \le \tau$. The third critical point is negative real (for τ sufficiently small). We denote this critical point by $\lambda_0(\chi, \tau)$ for any values of χ and τ for which $\lambda_\pm(\chi, \tau)$ are defined. Since τ is nonzero, as $\lambda \to \infty$, $\Re(\varphi(\lambda; \chi, \tau))$ is dominated by $\Re(i\lambda^2\tau)$. As the local behavior near ξ and ξ^* is topologically unchanged, the zero level curves must be topologically the same as in the case $\tau = 0$ with the addition of an unbounded curve that, for large $|\lambda|$, is approximately parallel to the imaginary axis. See the right panel in Figure 10.
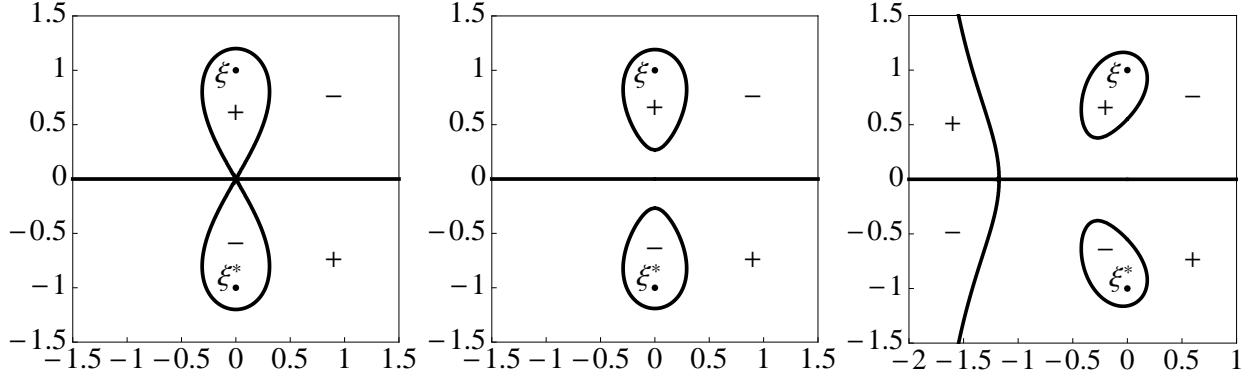

FIGURE 10. Signature charts of $\Re(\varphi(\lambda; \chi, \tau))$ in the complex λ-plane for $\xi = i$. *Left:* $(\chi, \tau) = (2, 0)$. *Center:* $(\chi, \tau) = (2.05, 0)$. *Right:* $(\chi, \tau) = (2.25, 0.6)$. The left panel illustrates the topology of the zero level lines for general $\xi = \alpha + i\beta$ if $\chi = \frac{2}{\beta}$ and $\tau = 0$, the center panel illustrates the general topology for $\chi > \frac{2}{\beta}$ and $\tau = 0$, and the right panel illustrates the general topology for $\chi > \frac{2}{\beta}$ and $\tau > 0$ with $|\tau|$ sufficiently small.

For fixed $\chi > \frac{2}{\beta}$, let $\tau \to +\infty$ (the argument as $\tau \to -\infty$ is analogous). Then, excluding shrinking neighborhoods of ξ and ξ^*, $\Re(\varphi(\lambda; \chi, \tau))$ is well approximated everywhere by $\Re(i\lambda^2\tau)$. This means that, with the possible exception of shrinking loops around ξ and ξ^*, the zero level curves of $\Re(\varphi(\lambda; \chi, \tau))$ are the real axis and an unbounded curve with real part approximately α. Furthermore, explicit calculation shows that $\Re(\varphi(a + i\beta; \chi, \tau)) > 0$ for $a < \alpha$ (for τ sufficiently large), and thus there are no closed loops on which $\Re(\varphi(\lambda; \chi, \tau)) > 0$ around ξ (or, by symmetry, around ξ^*).

Therefore, for fixed $\chi > \frac{2}{\beta}$, there is (at least one) topological change in the zero level lines of $\Re(\varphi(\lambda; \chi, \tau))$ as τ changes from zero to infinity. We show below that any (χ, τ) values before the first transition (starting from $\tau = 0$) are in the zero region. The topological change can happen in one of three ways, all of which occur for certain values of χ, τ, and ξ. The first way is for $\lambda_+(\chi, \tau)$ and $\lambda_-(\chi, \tau)$ to coincide on the real axis at a point distinct from $\lambda_0(\chi, t)$. This transition is illustrated in the first panel in Figure 11 (as well as the first panel in Figure 10 in the special

case $\tau = 0$). We conjecture that, as τ increases from this configuration, a single band will open in the model Riemann-Hilbert problem. This suggests a transition from the zero region to a region in which the solution to (1.1) is nonzero and non-oscillatory. A necessary algebraic condition for this to occur is for the discriminant of (3.5) to be zero, which is equivalent to

$$(16\alpha^4\beta^2 + 32\alpha^2\beta^4 + 16\beta^6)\tau^4 + (32\alpha^3\beta^2\chi - 16\alpha^3\beta + 32\alpha\beta^4\chi - 144\alpha\beta^3)\tau^3$$

(3.7)
$$+(24\alpha^2\beta^2\chi^2 - 24\alpha^2\beta\chi + 8\beta^4\chi^2 - 72\beta^3\chi + 108\beta^2)\tau^2$$

$$+(8\alpha\beta^2\chi^3 - 12\alpha\beta\chi^2)\tau + (\beta^2\chi^4 - 2\beta\chi^3) = 0.$$

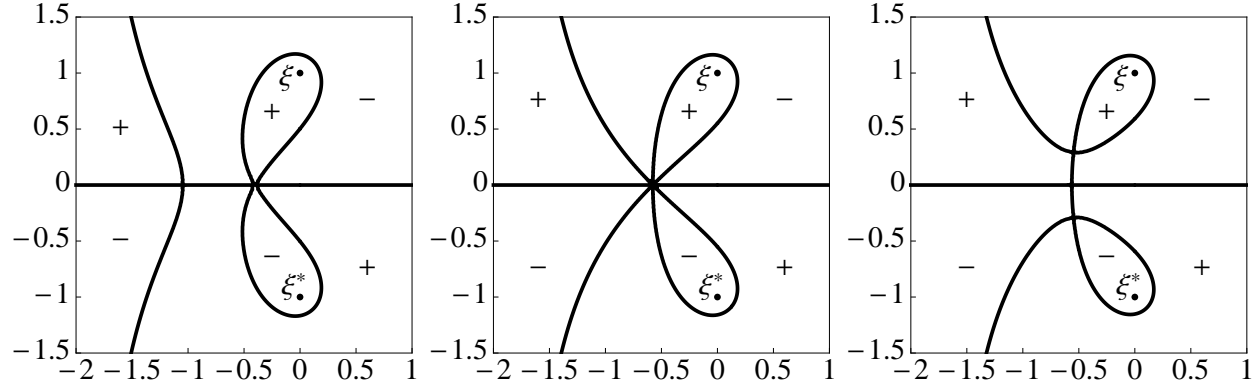If $\xi = i$, this simplifies to (1.7), a quadratic relation in τ^2.

FIGURE 11. Signature charts of $\Re(\varphi(\lambda; \chi, \tau))$ in the complex λ-plane for $\xi = i$. *Left:* $(\chi, \tau) \approx (2.2, 0.595)$. *Center:* $(\chi, \tau) = (\frac{9}{4}, \frac{3\sqrt{3}}{8})$. *Right:* $(\chi, \tau) \approx (2.3, 0.649)$. The left panel illustrates the boundary between the zero region with $\chi > 0$ and what we conjecture is a nonzero non-oscillatory region. The right panel illustrates the boundary between the zero region with $\chi > 0$ and what we conjecture is a nonzero single-phase region. The center panel illustrates the single point lying at the corner of the three different regions.

The second way the topological change can occur is if $\lambda_+(\chi, \tau)$, $\lambda_-(\chi, \tau)$, and $\lambda_0(\chi, \tau)$ all coincide. This is illustrated in the second panel in Figure 11. This double-critical behavior appears to correspond with a point at the corner of three different regions. If $\alpha = 0$, a necessary condition for this triple critical point is the discriminant of (3.7) must be zero, which occurs exactly (for $\tau > 0$) at the critical point

(3.8)
$$(\chi_c, \tau_c) = \left(\frac{9}{4\beta}, \frac{3\sqrt{3}}{8\beta^2} \right).$$

The third way for the topological change to occur, illustrated in the third panel in Figure 11, is when $\lambda_+(\chi, \tau)$ and $\lambda_-(\chi, \tau)$ simultaneously intersect a zero level line of $\Re(\varphi(\lambda; \chi, \tau))$ off the real axis. We expect this to correspond to an opening of two bands in the model Riemann-Hilbert problem and a transition between the zero region and a region in which the solution to (1.1) has single-phase oscillations with period of order n^{-1}. A necessary algebraic condition for this transition is the explicit (although transcendental) algebro-logarithmic relation (1.11). In Figure 6 we illustrate the boundary of the zero region computed using (3.7) and (1.11) for $\xi = i$ and $\xi = \frac{1}{2} + 2i$.

At this point we have proven the existence of a connected open region in the $\chi\tau$-plane containing the ray $\{(\chi, \tau) : \chi > \frac{2}{\beta}, \tau = 0\}$ such that

- The point $\lambda = \xi$ is enclosed by a simple loop on which $\Re(\varphi(\lambda; \chi, \tau)) = 0$. For λ immediately outside this loop $\Re(\varphi(\lambda; \chi, \tau)) < 0$, and for λ immediately inside this loop $\Re(\varphi(\lambda; \chi, \tau)) > 0$.
- The point $\lambda = \xi^*$ is enclosed by a simple loop on which $\Re(\varphi(\lambda; \chi, \tau)) = 0$. For λ immediately outside this loop $\Re(\varphi(\lambda; \chi, \tau)) > 0$, and for λ immediately inside this loop $\Re(\varphi(\lambda; \chi, \tau)) < 0$.

We denote the maximal region satisfying these conditions $\mathcal{Z}_+$. Furthermore, if $(\chi, \tau) \in \mathcal{Z}_+$, then it is immediate from (1.8) and (3.3) that $(-\chi, -\tau)$ has complementary properties:

- The point $\lambda = \xi$ is enclosed by a simple loop on which $\Re(\widetilde{\varphi}(\lambda; -\chi, -\tau)) = 0$. For λ immediately outside this loop $\Re(\widetilde{\varphi}(\lambda; -\chi, -\tau)) > 0$, and for λ immediately inside this loop $\Re(\widetilde{\varphi}(\lambda; -\chi, -\tau)) < 0$.
- The point $\lambda = \xi^*$ is enclosed by a simple loop on which $\Re(\widetilde{\varphi}(\lambda; -\chi, -\tau)) = 0$. For λ immediately outside this loop $\Re(\widetilde{\varphi}(\lambda; -\chi, -\tau)) < 0$, and for λ immediately inside this loop $\Re(\widetilde{\varphi}(\lambda; -\chi, -\tau)) > 0$.

We denote this complementary region by $\mathcal{Z}_-$, and we call $\mathcal{Z} := \mathcal{Z}_+ \cup \mathcal{Z}_-$ the *zero region*. We now use nonlinear steepest-descent analysis to show that $\psi^{[2n]}(x, t)$ is exponentially close to zero in the zero region as $n \to \infty$.

If $\chi > 0$, we denote the bounded region in the λ-plane containing ξ in which $\Re(\varphi(\lambda; \chi, \tau)) > 0$ by D_ξ, and the bounded region containing ξ^* in which $\Re(\varphi(\lambda; \chi, \tau)) < 0$ by D_{ξ^*}. Similarly, if $\chi < 0$, we denote the bounded region in the λ-plane containing ξ in which $\Re(\varphi(\lambda; \chi, \tau)) < 0$ by D_ξ, and the bounded region containing ξ^* in which $\Re(\varphi(\lambda; \chi, \tau)) > 0$ by D_{ξ^*}. Recall that the jump for $\mathbf{N}^{[n]}(\lambda; \chi, \tau)$ is defined on the loop ∂D_0 enclosing both ξ and ξ^*. The next step in the analysis is to deform the jump contour from ∂D_0 to $\partial D_\xi \cup \partial D_{\xi^*}$. Define

$$(3.9) \qquad \mathbf{O}^{[n]}(\lambda; \chi, \tau) := \begin{cases} \mathbf{N}^{[n]}(\lambda; \chi, \tau)\mathbf{V}_{\mathbf{N}}^{[n]}(\lambda; \chi, \tau), & \lambda \in D_0 \cap (D_\xi \cup D_{\xi^*})^{\mathsf{c}}, \\ \mathbf{N}^{[n]}(\lambda; \chi, \tau)\mathbf{V}_{\mathbf{N}}^{[n]}(\lambda; \chi, \tau)^{-1}, & \lambda \in (D_\xi \cup D_{\xi^*}) \cap D_0^{\mathsf{c}}, \\ \mathbf{N}^{[n]}(\lambda; \chi, \tau), & \text{otherwise.} \end{cases}$$

Then, orienting ∂D_ξ and ∂D_{ξ^*} clockwise, the function $\mathbf{O}^{[n]}(\lambda; \chi, \tau)$ is analytic for $\lambda \notin \partial D_\xi \cup \partial D_{\xi^*}$, satisfies $\mathbf{O}_+^{[n]}(\lambda; \chi, \tau) = \mathbf{O}_-^{[n]}(\lambda; \chi, \tau)\mathbf{V}_{\mathbf{O}}^{[n]}(\lambda; \chi, \tau)$ for $\lambda \in \partial D_\xi \cup \partial D_{\xi^*}$, where $\mathbf{V}_{\mathbf{O}}^{[n]}(\lambda; \chi, \tau) = \mathbf{V}_{\mathbf{N}}^{[n]}(\lambda; \chi, \tau)$, and $\mathbf{O}^{[n]}(\lambda; \chi, \tau) \to \mathbb{I}$ as $\lambda \to \infty$. Now observe we have the following four factorizations:

$$(3.10) \qquad \mathbf{S}^{-1} = \begin{pmatrix} 1 & \frac{c_2^*}{c_1} \\ 0 & 1 \end{pmatrix} \begin{pmatrix} \frac{|\mathbf{c}|}{c_1} & 0 \\ 0 & \frac{c_1}{|\mathbf{c}|} \end{pmatrix} \begin{pmatrix} 1 & 0 \\ -\frac{c_2}{c_1} & 1 \end{pmatrix} \qquad (\text{use for } \lambda \in \partial D_\xi, \ \chi > 0),$$

$$(3.11) \qquad \mathbf{S}^{-1} = \begin{pmatrix} 1 & 0 \\ -\frac{c_2}{c_1^*} & 1 \end{pmatrix} \begin{pmatrix} \frac{c_1^*}{|\mathbf{c}|} & 0 \\ 0 & \frac{|\mathbf{c}|}{c_1^*} \end{pmatrix} \begin{pmatrix} 1 & \frac{c_2^*}{c_1^*} \\ 0 & 1 \end{pmatrix} \qquad (\text{use for } \lambda \in \partial D_{\xi^*}, \ \chi > 0),$$

$$(3.12) \qquad \widetilde{\mathbf{S}}^{-1} = \begin{pmatrix} 1 & 0 \\ \frac{c_1^*}{c_2} & 1 \end{pmatrix} \begin{pmatrix} \frac{c_2}{|\mathbf{c}|} & 0 \\ 0 & \frac{|\mathbf{c}|}{c_2} \end{pmatrix} \begin{pmatrix} 1 & -\frac{c_1}{c_2} \\ 0 & 1 \end{pmatrix} \qquad (\text{use for } \lambda \in \partial D_\xi, \ \chi < 0),$$

$$(3.13) \qquad \widetilde{\mathbf{S}}^{-1} = \begin{pmatrix} 1 & -\frac{c_1^*}{c_2^*} \\ 0 & 1 \end{pmatrix} \begin{pmatrix} \frac{|\mathbf{c}|}{c_2^*} & 0 \\ 0 & \frac{c_2^*}{|\mathbf{c}|} \end{pmatrix} \begin{pmatrix} 1 & 0 \\ \frac{c_1^*}{c_2^*} & 1 \end{pmatrix} \qquad (\text{use for } \lambda \in \partial D_{\xi^*}, \ \chi < 0).$$

For convenience we indicate when we will use each factorization; of course each relation is an algebraic identity that holds independent of λ or χ. First, suppose $\chi > 0$. We define four simple clockwise-oriented loops $\Sigma_\xi^{(\text{out})}$, $\Sigma_\xi^{(\text{in})}$, $\Sigma_{\xi^*}^{(\text{out})}$, and $\Sigma_{\xi^*}^{(\text{in})}$ such that:

- $\Sigma_\xi^{(\text{out})}$ encloses D_ξ and lies entirely in the region in which $\Re(\varphi(\lambda; \chi, \tau)) < 0$.
- $\Sigma_\xi^{(\text{in})}$ encloses ξ and lies entirely in D_ξ (so that $\Re(\varphi(\lambda; \chi, \tau)) > 0$).
- $\Sigma_{\xi^*}^{(\text{out})}$ encloses D_{ξ^*} and lies entirely in the region in which $\Re(\varphi(\lambda; \chi, \tau)) > 0$.

- $\Sigma_{\xi^*}^{(\mathrm{in})}$ encloses ξ^* and lies entirely in D_{ξ^*} (so that $\Re(\varphi(\lambda;\chi,\tau)) < 0$).

Also define the following four annular regions:

- $L_\xi^{(\mathrm{out})}$ is bounded by ∂D_ξ and $\Sigma_\xi^{(\mathrm{out})}$.
- $L_\xi^{(\mathrm{in})}$ is bounded by ∂D_ξ and $\Sigma_\xi^{(\mathrm{in})}$.
- $L_{\xi^*}^{(\mathrm{out})}$ is bounded by ∂D_{ξ^*} and $\Sigma_{\xi^*}^{(\mathrm{out})}$.
- $L_{\xi^*}^{(\mathrm{in})}$ is bounded by ∂D_{ξ^*} and $\Sigma_{\xi^*}^{(\mathrm{in})}$.

For $(\chi,\tau) \in \mathcal{Z}$ and $\chi > 0$, define

$$(3.14) \qquad \mathbf{P}^{[n]}(\lambda;\chi,\tau) := \begin{cases} \mathbf{O}^{[n]}(\lambda;\chi,\tau) \begin{pmatrix} 1 & \frac{c_2^*}{c_1}e^{-2n\varphi(\lambda;\chi,\tau)} \\ 0 & 1 \end{pmatrix}, & \lambda \in L_\xi^{(\mathrm{in})}, \\[12pt] \mathbf{O}^{[n]}(\lambda;\chi,\tau) \begin{pmatrix} 1 & 0 \\ -\frac{c_2}{c_1}e^{2n\varphi(\lambda;\chi,\tau)} & 1 \end{pmatrix}^{-1}, & \lambda \in L_\xi^{(\mathrm{out})}, \\[12pt] \mathbf{O}^{[n]}(\lambda;\chi,\tau) \begin{pmatrix} 1 & 0 \\ -\frac{c_2}{c_1^*}e^{2n\varphi(\lambda;\chi,\tau)} & 1 \end{pmatrix}, & \lambda \in L_{\xi^*}^{(\mathrm{in})}, \\[12pt] \mathbf{O}^{[n]}(\lambda;\chi,\tau) \begin{pmatrix} 1 & \frac{c_2^*}{c_1^*}e^{-2n\varphi(\lambda;\chi,\tau)} \\ 0 & 1 \end{pmatrix}^{-1}, & \lambda \in L_{\xi^*}^{(\mathrm{out})}, \\[12pt] \mathbf{O}^{[n]}(\lambda;\chi,\tau), & \text{otherwise.} \end{cases}$$

Then $\mathbf{P}^{[n]}(\lambda;\chi,\tau)$ is analytic for $\lambda \notin \partial D_\xi \cup \partial D_{\xi^*} \cup \Sigma_\xi^{(\mathrm{out})} \cup \Sigma_\xi^{(\mathrm{in})} \cup \Sigma_{\xi^*}^{(\mathrm{out})} \cup \Sigma_{\xi^*}^{(\mathrm{in})}$, has the normalization $\mathbf{P}^{[n]}(\lambda;\chi,\tau) \to \mathbb{I}$ as $\lambda \to \infty$, and has the jumps $\mathbf{P}_+^{[n]}(\lambda;\chi,\tau) = \mathbf{P}_-^{[n]}(\lambda;\chi,\tau)\mathbf{V}_{\mathbf{P}}^{[n]}(\lambda;\chi,\tau)$, where

$$(3.15) \qquad \mathbf{V}_{\mathbf{P}}^{[n]}(\lambda;\chi,\tau) := \begin{cases} \begin{pmatrix} 1 & \frac{c_2^*}{c_1}e^{-2n\varphi(\lambda;\chi,\tau)} \\ 0 & 1 \end{pmatrix}, & \lambda \in \Sigma_\xi^{(\mathrm{in})}, \\[12pt] \begin{pmatrix} \frac{|\mathbf{c}|}{c_1} & 0 \\ 0 & \frac{c_1}{|\mathbf{c}|} \end{pmatrix}, & \lambda \in \partial D_\xi, \\[12pt] \begin{pmatrix} 1 & 0 \\ -\frac{c_2}{c_1}e^{2n\varphi(\lambda;\chi,\tau)} & 1 \end{pmatrix}, & \lambda \in \Sigma_\xi^{(\mathrm{out})}, \\[12pt] \begin{pmatrix} 1 & 0 \\ -\frac{c_2}{c_1^*}e^{2n\varphi(\lambda;\chi,\tau)} & 1 \end{pmatrix}, & \lambda \in \Sigma_{\xi^*}^{(\mathrm{in})}, \\[12pt] \begin{pmatrix} \frac{c_1^*}{|\mathbf{c}|} & 0 \\ 0 & \frac{|\mathbf{c}|}{c_1^*} \end{pmatrix}, & \lambda \in \partial D_{\xi^*}, \\[12pt] \begin{pmatrix} 1 & \frac{c_2^*}{c_1^*}e^{-2n\varphi(\lambda;\chi,\tau)} \\ 0 & 1 \end{pmatrix}, & \lambda \in \Sigma_{\xi^*}^{(\mathrm{out})}. \end{cases}$$

The jumps for $\mathbf{P}^{[n]}(\lambda;\chi,\tau)$ on the contours $\Sigma_\xi^{(\mathrm{out})}$, $\Sigma_\xi^{(\mathrm{in})}$, $\Sigma_{\xi^*}^{(\mathrm{out})}$, and $\Sigma_{\xi^*}^{(\mathrm{in})}$ all decay exponentially to $\mathbb{I}$ as $n \to \infty$. Thus we define $\mathbf{Q}(\lambda;\chi,\tau)$ as the n-independent solution to the following Riemann-Hilbert problem:

Riemann-Hilbert Problem 2 (The model problem in the zero region with $\chi > 0$). *Fix a pair of nonzero complex numbers (c_1, c_2), along with a pair of real numbers $(\chi,\tau) \in \mathcal{Z}$ with $\chi > 0$. Determine the unique 2×2 matrix $\mathbf{Q}(\lambda;\chi,\tau)$ with the following properties:*

> ***Analyticity:*** *$\mathbf{Q}(\lambda;\chi,\tau)$ is analytic for $\lambda \in \mathbb{C}$ except on $\partial D_\xi \cup \partial D_{\xi^*}$, where it achieves continuous boundary values.*

Jump condition: *The boundary values taken by $\mathbf{Q}(\lambda; \chi, \tau)$ are related by the jump conditions $\mathbf{Q}_+(\lambda; \chi, \tau) = \mathbf{Q}_-(\lambda; \chi, \tau)\mathbf{V_Q}(\lambda; \chi, \tau)$, where*

(3.16)
$$\mathbf{V_Q}(\lambda; \chi, \tau) := \begin{cases} \begin{bmatrix} \frac{|\mathbf{c}|}{c_1} & 0 \\ 0 & \frac{c_1}{|\mathbf{c}|} \end{bmatrix}, & \lambda \in \partial D_\xi, \\[20pt] \begin{bmatrix} \frac{c_1^*}{|\mathbf{c}|} & 0 \\ 0 & \frac{|\mathbf{c}|}{c_1^*} \end{bmatrix}, & \lambda \in \partial D_{\xi^*}. \end{cases}$$

Normalization: *As $\lambda \to \infty$, the matrix $\mathbf{Q}(\lambda; \chi, \tau)$ satisfies the condition*

(3.17)
$$\mathbf{Q}(\lambda; \chi, \tau) = \mathbb{I} + \mathcal{O}(\lambda^{-1})$$

with the limit being uniform with respect to direction.

This Riemann-Hilbert problem reduces to two scalar problems, and as such can be solved explicitly using the Plemelj formula. However, we will not need the exact formula, only that $\mathbf{Q}(\lambda; \chi, \tau)$ is diagonal:

(3.18)
$$\mathbf{Q}(\lambda; \chi, \tau) \equiv \begin{pmatrix} Q_{11}(\lambda; \chi, \tau) & 0 \\ 0 & Q_{22}(\lambda; \chi, \tau) \end{pmatrix}.$$

Finally, we define the error function by the ratio

(3.19)
$$\mathbf{R}^{[n]}(\lambda; \chi, \tau) := \mathbf{P}^{[n]}(\lambda; \chi, \tau)\mathbf{Q}(\lambda; \chi, \tau)^{-1}.$$

The jumps across ∂D_ξ and ∂D_{ξ^*} cancel exactly. Therefore, $\mathbf{R}^{[n]}(\lambda; \chi, \tau)$ is analytic for $\lambda \notin \Sigma_\xi^{(\text{in})} \cup \Sigma_\xi^{(\text{out})} \cup \Sigma_{\xi^*}^{(\text{in})} \cup \Sigma_{\xi^*}^{(\text{out})}$, $\mathbf{R}^{[n]}(\lambda; \chi, \tau) \to \mathbb{I}$ as $\lambda \to \infty$, and $\mathbf{R}_+^{[n]}(\lambda; \chi, \tau) = \mathbf{R}_-^{[n]}(\lambda; \chi, \tau)\mathbf{V_R}^{[n]}(\lambda; \chi, \tau)$, where

(3.20)
$$\mathbf{V_R}^{[n]}(\lambda; \chi, \tau) = \mathbf{Q}_-(\lambda; \chi, \tau)\mathbf{V_P}^{[n]}(\lambda; \chi, \tau)\mathbf{Q}_+(\lambda; \chi, \tau)^{-1}.$$

Therefore, the jump matrices for $\mathbf{R}^{[n]}(\lambda; \chi, \tau)$ are exponentially close to the identity matrix as $n \to \infty$. From standard nonlinear steepest-descent analysis (see, for instance, [13] or [11, Appendix B]), there is a constant $d > 0$ such that $\mathbf{R}^{[n]}(\lambda; \chi, \tau) = \mathbb{I} + \mathcal{O}(e^{-dn})$ uniformly in λ and uniformly in (χ, τ) bounded a fixed distance away from the edge of the zero region. This implies that $\mathbf{P}^{[n]}(\lambda; \chi, \tau)$ is exponentially close to $\mathbf{Q}(\lambda; \chi, \tau)$ as $n \to \infty$. Unwinding the transformations $\mathbf{M}^{[n]}(\lambda; \chi, \tau) \to \mathbf{N}^{[n]}(\lambda; \chi, \tau) \to \mathbf{O}^{[n]}(\lambda; \chi, \tau) \to \mathbf{P}^{[n]}(\lambda; \chi, \tau)$, for fixed $(\chi, \tau) \in \mathcal{Z}$ with $\chi > 0$, we have in particular

(3.21)
$$[\mathbf{M}^{[n]}(\lambda; n\chi, n\tau)]_{12} = \mathcal{O}(e^{-dn})$$

for some constant $d > 0$ uniformly in λ. Thus, from (1.5), for fixed $(\chi, \tau) \in \mathcal{Z}$ with $\chi > 0$, (1.12) holds for some constant $d > 0$. The analysis for $(\chi, \tau) \in \mathcal{Z}$ with $\chi < 0$ follows exactly the same logic, only starting from the factorizations (3.12)–(3.13) instead of (3.10)–(3.11). This concludes the proof of Theorem 1 and the asymptotic description of the zero region.

4. THE NEAR-FIELD LIMIT AND THE PAINLEVÉ-III HIERARCHY

We now prove Theorem 2. Our first move is to obtain an n-independent Riemann-Hilbert problem whose solution is a good approximation of $\mathbf{M}^{[n]}(\lambda; x, t)$ in a suitable rescaling near $(x, t) = (0, 0)$. Recall the near-field scalings $X := nx$, $T := n^2 t$ (see (1.13)). We also scale the spectral parameter λ:

(4.1)
$$\Lambda := n^{-1}\lambda.$$

With this scaling in mind we recall that the radius of the jump contour D_0 for $\mathbf{M}^{[n]}(\lambda; x, t)$ is arbitrary (as long as it encloses ξ). Thus we choose ∂D_0 to be a circle of radius n centered at

the origin (and hence $|\Lambda| = 1$). Applying these scalings for x, t, and λ to the jump matrix for $\mathbf{M}^{[n]}(\lambda; x, t)$ in (1.3) gives

(4.2)
$$e^{-i(\lambda x + \lambda^2 t)\sigma_3} \mathbf{S} \left(\frac{\lambda - \xi}{\lambda - \xi^*} \right)^{n\sigma_3} \mathbf{S}^{-1} e^{i(\lambda x + \lambda^2 t)\sigma_3} \bigg|_{x = n^{-1}X,\, t = n^{-2}T,\, \lambda = n\Lambda} =$$
$$\left(\mathbb{I} + \mathcal{O}(n^{-1}) \right) e^{-i(\Lambda X + \Lambda^2 T)\sigma_3} \mathbf{S} e^{-2i\beta\Lambda^{-1}\sigma_3} \mathbf{S}^{-1} e^{i(\Lambda X + \Lambda^2 T)\sigma_3}.$$

Neglecting the terms of $\mathcal{O}(n^{-1})$, we arrive (formally) at the near-field Riemann-Hilbert problem.

Riemann-Hilbert Problem 3 (The near-field problem). *Let $(X, T) \in \mathbb{R}^2$ be fixed but arbitrary parameters. Find the unique 2×2 matrix-valued function $\mathbf{A}(\Lambda; X, T)$ with the following properties:*

> *__Analyticity:__ $\mathbf{A}(\Lambda; X, T)$ is analytic in Λ for $|\Lambda| \neq 1$, and it takes continuous boundary values from the interior and exterior of $|\Lambda| = 1$.*
>
> *__Jump condition:__ The boundary values on the jump contour (oriented clockwise) follow the relation*

(4.3)
$$\mathbf{A}_+(\Lambda; X, T) = \mathbf{A}_-(\Lambda; X, T) e^{-i(\Lambda X + \Lambda^2 T)\sigma_3} \mathbf{S} e^{-2i\beta\Lambda^{-1}\sigma_3} \mathbf{S}^{-1} e^{i(\Lambda X + \Lambda^2 T)\sigma_3}, \quad |\Lambda| = 1.$$

> *__Normalization:__ $\mathbf{A}(\Lambda; X, T) \to \mathbb{I}$ as $\Lambda \to \infty$.*

If $(c_1, c_2) = (1, \pm 1)$ and $\xi = i$, then Riemann-Hilbert Problem 3 is exactly Riemann-Hilbert Problem 3 in [7] used to define $\Psi(X, T; (1, \pm 1))$. We now define

(4.4)
$$\Psi(X, T; \mathbf{c}) := 2i \lim_{\Lambda \to \infty} \Lambda [\mathbf{A}(\Lambda; X, T)]_{12}.$$

As we show in Theorem 2, this function $\Psi(X, T; \mathbf{c})$ is the scaled limit of $\psi^{[2n]}(x, t; \mathbf{c})$ in the near field. From here on we assume $\xi = i$.

4.1. **The function $\Psi(X, T)$ and the NLS equation: Proof of Theorem 2(a).** To prove (1.14) we follow the standard argument used in [7, Theorem 1]. To measure the difference between Riemann-Hilbert Problem 1 (appropriately scaled) and Riemann-Hilbert Problem 3, define the ratio matrix

(4.5)
$$\mathbf{F}(\Lambda; X, T; \mathbf{c}) := \mathbf{M}^{[n]} \left(n\Lambda; \frac{X}{n}, \frac{T}{n^2}; \mathbf{c} \right) \mathbf{A}(\Lambda; X, T; \mathbf{c})^{-1}.$$

Then $\mathbf{F}(\Lambda; X, T)$ is analytic for $|\Lambda| \neq 1$, whereas for $|\Lambda| = 1$ we have

(4.6)
$$\mathbf{F}_+(\Lambda; X, T) = \mathbf{F}_-(\Lambda; X, T) \mathbf{A}_-(\Lambda; X, T)(\mathbb{I} + \mathcal{O}(n^{-1})) \mathbf{A}_-(\Lambda; X, T)^{-1}$$
$$= \mathbf{F}_-(\Lambda; X, T)(\mathbb{I} + \mathcal{O}(n^{-1})).$$

Here the first line follows from (4.2), while the second line follows from the boundedness of $\mathbf{A}(\Lambda; X, T)$ and the fact that $\det \mathbf{A}(\Lambda; X, T) \equiv 1$. Since we also have $\mathbf{F}(\Lambda; X, T) \to \mathbb{I}$ as $\Lambda \to \infty$, the function $\mathbf{F}(\Lambda; X, T)$ satisfies a small-norm Riemann-Hilbert problem, from which it follows [13] that

(4.7)
$$\mathbf{F}(\Lambda; X, T) = \mathbb{I} + \mathcal{O}(n^{-1})$$

uniformly for compact regions in the XT-plane. Starting from (1.5),

(4.8)
$$\frac{1}{n} \psi^{[2n]} \left(\frac{X}{n}, \frac{T}{n^2} \right) = \frac{2i}{n} \lim_{\lambda \to \infty} \lambda \left[\mathbf{M}^{[n]} \left(\lambda; \frac{X}{n}, \frac{T}{n^2} \right) \right]_{12}$$
$$= \frac{2i}{n} \lim_{\Lambda \to \infty} n\Lambda \left([\mathbf{F}(\Lambda; X, T)]_{11} [\mathbf{A}(\Lambda; X, T)]_{12} + [\mathbf{F}(\Lambda; X, T)]_{12} [\mathbf{A}(\Lambda; X, T)]_{22} \right)$$
$$= 2i \lim_{\Lambda \to \infty} \Lambda [\mathbf{A}(\Lambda; X, T)]_{12} + \mathcal{O}(n^{-1})$$
$$= \Psi(X, T) + \mathcal{O}(n^{-1})$$

uniformly in X and T chosen from compact sets.

To prove that $\Psi(X, T; \mathbf{c})$ satisfies the nonlinear Schrödinger equation, define

$$(4.9) \qquad \mathbf{K}(\Lambda; X, T) := \mathbf{A}(\Lambda; X, T)e^{-i(\Lambda X + \Lambda^2 T)\sigma_3}.$$

Then, following the proof of [7, Proposition 3] with their matrix $\mathbf{Q} = \frac{1}{\sqrt{2}}\begin{bmatrix} 1 & -1 \\ 1 & 1 \end{bmatrix}$ replaced with the more general matrix $\mathbf{S}$ (indeed, $\mathbf{S} = \mathbf{Q}$ if $\mathbf{c} = (1, 1)$), the function $\mathbf{K}(\Lambda; X, T)$ satisfies the system of overdetermined ordinary differential equations

$$(4.10) \qquad \begin{aligned} \frac{\partial \mathbf{K}}{\partial X}(\Lambda; X, T) &= \begin{bmatrix} -i\Lambda & \Psi(X, T) \\ -\Psi(X, T) & i\Lambda \end{bmatrix} \mathbf{K}(\Lambda; X, T), \\ \frac{\partial \mathbf{K}}{\partial T}(\Lambda; X, T) &= \begin{bmatrix} -i\Lambda^2 + \frac{i}{2}|\Psi(X, T)|^2 & \Lambda\Psi(X, T) + \frac{i}{2}\Psi_X(X, T) \\ -\Lambda\Psi(X, T)^* + \frac{i}{2}\Psi_X(X, T)^* & i\Lambda^2 - \frac{i}{2}|\Psi(X, T)|^2 \end{bmatrix} \mathbf{K}(\Lambda; X, T), \end{aligned}$$

which is simply the Lax pair (2.1) with ψ, x, t, and λ replaced by Ψ, X, T, and Λ, respectively. This means (1.15) is equivalent to the condition $\mathbf{K}_{XT}(\Lambda; X, T) = \mathbf{K}_{TX}(\Lambda; X, T)$, and so $\Psi(X, T)$ satisfies (1.15). This completes the proof of Theorem 2(a).

4.2. The function $\Psi(X, T)$ and the P_{III} hierarchy: Proof of Theorem 2(b).
In [7, §3.2.1] it is shown that $\Psi(X, T; (1, \pm 1))$ satisfies (1.16) by deriving a Lax pair in Λ and X for the function

$$(4.11) \qquad \mathbf{B}(\Lambda; X, T)e^{-i(\Lambda X + \Lambda^2 T + 2\Lambda^{-1})\sigma_3},$$

where

$$(4.12) \qquad \mathbf{B}(\Lambda; X, T) := \begin{cases} \mathbf{A}(\Lambda; X, T)e^{-i(\Lambda X + \Lambda^2 T)\sigma_3}\mathbf{S}^{-1}e^{i(\Lambda X + \Lambda^2 T)\sigma_3}, & |\Lambda| < 1, \\ \mathbf{A}(\Lambda; X, T)e^{2i\Lambda^{-1}\sigma_3}, & |\Lambda| > 1. \end{cases}$$

The derivation depends on the fact that the jump for this function across the unit circle is constant, but not on the particular constant jump matrix. Since we have

$$(4.13) \qquad (\mathbf{B}(\Lambda; X, T)e^{-i(\Lambda X + \Lambda^2 T + 2\Lambda^{-1})\sigma_3})_+ = (\mathbf{B}(\Lambda; X, T)e^{-i(\Lambda X + \Lambda^2 T + 2\Lambda^{-1})\sigma_3})_- \mathbf{S}^{-1}, \quad |\Lambda| = 1,$$

the derivation in [7] goes through unchanged, and $\Psi(X, T; \mathbf{c})$ satisfies (1.16) for general $\mathbf{c} \in (\mathbb{C}^*)^2$. We now calculate $\Psi(0, 0; \mathbf{c})$ and $\Psi_X(0, 0; \mathbf{c})$.

Lemma 1. *For any* $\mathbf{c} = (c_1, c_2) \in (\mathbb{C}^*)^2$ *and* $\xi = i$, $\Psi(0, 0; \mathbf{c}) = 8\frac{c_1 c_2^*}{|\mathbf{c}|^2}$.

Proof. Using the (Riemann-Hilbert) properties of $\mathbf{A}(\Lambda; X, T)$, we see that $\mathbf{B}(\Lambda; X, T)$ defined in (4.12) is unimodular and analytic for $\Lambda \neq 0$ away from $|\Lambda| = 1$, and has the property $\mathbf{B}(\Lambda; X, T) \to \mathbb{I}$ as $\Lambda \to \infty$. The jump condition satisfied by $\mathbf{B}(\Lambda; X, T)$ is

$$(4.14) \qquad \mathbf{B}_+(\Lambda; X, T) = \mathbf{B}_-(\Lambda; X, T)e^{-i(\Lambda X + \Lambda^2 T + 2\Lambda^{-1})\sigma_3}\mathbf{S}^{-1}e^{i(\Lambda X + \Lambda^2 T + 2\Lambda^{-1})\sigma_3}, \quad |\Lambda| = 1.$$

Moreover, since $e^{2i\Lambda^{-1}\sigma_3} = \mathbb{I} + 2i\sigma_3\Lambda^{-1} + \mathcal{O}(\Lambda^{-2})$ as $\Lambda \to \infty$, the identity (4.4) implies that we recover $\Psi(X, T; \mathbf{c})$ via the limit

$$(4.15) \qquad \Psi(X, T; \mathbf{c}) = 2i\lim_{\Lambda \to \infty} \Lambda[\mathbf{B}(\Lambda; X, T)]_{12}.$$

When $(X, T) = (0, 0)$, we have the explicit formula

$$(4.16) \qquad \mathbf{B}(\Lambda; 0, 0) = \begin{cases} \mathbf{S}, & |\Lambda| < 1, \\ \mathbf{S}e^{-2i\Lambda^{-1}\sigma_3}\mathbf{S}^{-1}e^{2i\Lambda^{-1}\sigma_3}, & |\Lambda| > 1. \end{cases}$$

Then, as $\Lambda \to \infty$,

$$(4.17) \qquad \begin{aligned} \mathbf{S}e^{-2i\Lambda^{-1}\sigma_3}\mathbf{S}^{-1}e^{2i\Lambda^{-1}\sigma_3} &= \mathbf{S}\left(\mathbb{I} - 2i\Lambda^{-1}\sigma_3 + \mathcal{O}(\Lambda^{-2})\right)\mathbf{S}^{-1}\left(\mathbb{I} + 2i\Lambda^{-1}\sigma_3 + \mathcal{O}(\Lambda^{-2})\right) \\ &= \mathbb{I} + 2i(\sigma_3 - \mathbf{S}\sigma_3\mathbf{S}^{-1})\Lambda^{-1} + \mathcal{O}(\Lambda^{-2}), \end{aligned}$$

and hence

$$(4.18) \qquad \Psi(0,0;\mathbf{c}) = -4\left[\sigma_3 - \mathbf{S}\sigma_3\mathbf{S}^{-1}\right]_{12} = 8\frac{c_1 c_2^*}{|\mathbf{c}|^2},$$

as asserted. $\qquad\square$

Lemma 2. *For any* $\mathbf{c} = (c_1, c_2) \in (\mathbb{C}^*)^2$ *and* $\xi = i$, $\Psi_X(0,0;\mathbf{c}) = 32\frac{c_1 c_2^*}{|\mathbf{c}|^4}(c_2 c_2^* - c_1 c_1^*)$.

Proof. We expand $\mathbf{B}(\Lambda; X, T)$ as

$$(4.19) \qquad \mathbf{B}(\Lambda; X, T) = \mathbb{I} + \frac{1}{\Lambda}\mathbf{B}_{-1}(X, T) + \frac{1}{\Lambda^2}\mathbf{B}_{-2}(X, T) + \mathcal{O}\left(\frac{1}{\Lambda^3}\right), \quad \Lambda \to \infty.$$

From (4.9) and (4.12),

$$(4.20) \qquad \mathbf{K}(\Lambda; X, T) = \mathbf{B}(\Lambda; X, T)e^{-i(\Lambda x + \Lambda^2 T + 2i\Lambda^{-1})\sigma_3}, \quad |\Lambda| > 1.$$

Inserting this expression into

$$(4.21) \qquad \mathbf{K}_T(\Lambda; X, T)\mathbf{K}(\Lambda; X, T)^{-1} = \begin{bmatrix} -i\Lambda^2 + \frac{i}{2}|\Psi(X, T)|^2 & \Lambda\Psi(X, T) + \frac{i}{2}\Psi_X(X, T) \\ -\Lambda\Psi(X, T)^* + \frac{i}{2}\Psi_X(X, T)^* & i\Lambda^2 - \frac{i}{2}|\Psi(X, T)|^2 \end{bmatrix}$$

and expanding as $\Lambda \to \infty$ shows

$$(4.22) \qquad \Psi_X(0,0;\mathbf{c}) = 4[\mathbf{B}_{-2}(0,0)]_{12} - 4[\mathbf{B}_{-1}(0,0)]_{12}[\mathbf{B}_{-1}(0,0)]_{22}.$$

From the formula (4.16) for $\mathbf{B}(\Lambda; 0, 0)$,

$$(4.23) \qquad [\mathbf{B}_{-2}(0,0)]_{12} = -\frac{8}{|\mathbf{c}|^2}c_1 c_2^*, \quad [\mathbf{B}_{-1}(0,0)]_{12} = -\frac{4i}{|\mathbf{c}|^2}c_1 c_2^*, \quad [\mathbf{B}_{-1}(0,0)]_{22} = -\frac{4i}{|\mathbf{c}|^2}c_2 c_2^*.$$

Combining (4.22) and (4.23) gives the desired result. $\qquad\square$

Now that $\Psi(0,0;\mathbf{c})$ and $\Psi_X(0,0;\mathbf{c})$ are known, higher derivatives $\frac{\partial^j \Psi}{\partial X^j}(0,0;\mathbf{c})$ can be found using (1.16). Our next step is to prove (1.18).

Lemma 3. $\Psi(-X, T; \mathbf{c}^*\sigma_1) = \Psi(X, T; \mathbf{c})$ *for any* $\mathbf{c} \in (\mathbb{C}^*)^2$.

Proof. Let $\mathbf{A}(\Lambda; X, T)$ be the unique solution of Riemann-Hilbert Problem 3 with given $\mathbf{c} = (c_1, c_2) \in (\mathbb{C}^*)^2$ and $(X, T) \in \mathbb{R}^2$, and hence

$$(4.24) \qquad 2i\left[\mathbf{A}(\Lambda; X, T; \mathbf{c})\right]_{12} = \frac{\Psi(X, T; \mathbf{c})}{\Lambda} + \mathcal{O}\left(\frac{1}{\Lambda^2}\right), \quad \Lambda \to \infty.$$

From the different representations given in (2.38) with $\mathbf{S} = \mathbf{S}(\mathbf{c})$ and $\widetilde{\mathbf{S}} = \widetilde{\mathbf{S}}(\mathbf{c})$ defined as in (1.4) and (2.37), it follows that the jump matrix

$$(4.25) \qquad \mathbf{V_A}(\Lambda; X, T; \mathbf{c}) := e^{-i(\Lambda X + \Lambda^2 T)\sigma_3}\mathbf{S}(\mathbf{c})e^{-2i\Lambda^{-1}\sigma_3}\mathbf{S}(\mathbf{c})^{-1}e^{i(\Lambda X + \Lambda^2 T)\sigma_3}$$

in (4.3) also has the representation

$$(4.26) \qquad \mathbf{V_A}(\Lambda; X, T; \mathbf{c}) = e^{-i(\Lambda X + \Lambda^2 T)\sigma_3}\widetilde{\mathbf{S}}(\mathbf{c})e^{2i\Lambda^{-1}\sigma_3}\widetilde{\mathbf{S}}(\mathbf{c})^{-1}e^{i(\Lambda X + \Lambda^2 T)\sigma_3}.$$

Using the identity

$$(4.27) \qquad \mathbf{S}(\sigma_1\mathbf{c}^*) = \frac{1}{|\mathbf{c}^*|}\begin{pmatrix} c_2^* & -c_1 \\ c_1^* & c_2 \end{pmatrix} = \sigma_3\frac{1}{|\mathbf{c}|}\begin{pmatrix} c_2^* & c_1 \\ -c_1^* & c_2 \end{pmatrix}\sigma_3 = \sigma_3\widetilde{\mathbf{S}}(\mathbf{c})\sigma_3,$$

we see that

$$(4.28) \qquad \begin{aligned} \mathbf{V_A}(-\Lambda; -X, T; \mathbf{c}^*\sigma_1) &= e^{-i(\Lambda X + \Lambda^2 T)\sigma_3}\mathbf{S}(\mathbf{c}^*\sigma_1)e^{2i\Lambda^{-1}\sigma_3}\mathbf{S}(\mathbf{c}^*\sigma_1)^{-1}e^{i(\Lambda X + \Lambda^2 T)\sigma_3} \\ &= \sigma_3 e^{-i(\Lambda X + \Lambda^2 T)\sigma_3}\widetilde{\mathbf{S}}(\mathbf{c})e^{2i\Lambda^{-1}\sigma_3}\widetilde{\mathbf{S}}(\mathbf{c})^{-1}e^{i(\Lambda X + \Lambda^2 T)\sigma_3}\sigma_3 \\ &= \sigma_3\mathbf{V_A}(\Lambda; X, T; \mathbf{c})\sigma_3. \end{aligned}$$

Thus, the matrix function $\widehat{\mathbf{A}}(\Lambda; X, T; \mathbf{c}) := \sigma_3 \mathbf{A}(-\Lambda; -X, T; \mathbf{c}^* \sigma_1) \sigma_3$ satisfies the jump condition

$$(4.29) \qquad \widehat{\mathbf{A}}_+(\Lambda; X, T; \mathbf{c}) = \widehat{\mathbf{A}}_-(\Lambda; X, T; \mathbf{c}) \mathbf{V_A}(\Lambda; X, T; \mathbf{c}), \quad |\Lambda| = 1,$$

which is exactly the jump condition (4.3) in Riemann-Hilbert Problem 3. Moreover, $\widehat{\mathbf{A}}(\Lambda; X, T; \mathbf{c})$ is well-defined and analytic away from $|\Lambda| = 1$, $\det \widehat{\mathbf{A}}(\Lambda; X, T; \mathbf{c}) = 1$ on its domain of definition, and $\widehat{\mathbf{A}}(\Lambda; X, T; \mathbf{c}) \to \mathbb{I}$ as $\Lambda \to \infty$. Therefore, $\widehat{\mathbf{A}}(\Lambda; X, T; \mathbf{c}) = \sigma_3 \mathbf{A}(-\Lambda; -X, T; \mathbf{c}^* \sigma_1) \sigma_3$ also solves Riemann-Hilbert Problem 3. The identity

$$(4.30) \qquad \mathbf{A}(\Lambda; X, T; \mathbf{c}) = \sigma_3 \mathbf{A}(-\Lambda; -X, T; \mathbf{c}^* \sigma_1) \sigma_3$$

follows from uniqueness of the solution to the Riemann-Hilbert problem. Using (4.30), we write

$$(4.31) \quad \Psi(-X, T; \mathbf{c}^* \sigma_1) = 2i \lim_{\Lambda \to \infty} \Lambda \left[\mathbf{A}(\Lambda; -X, T; \mathbf{c}^* \sigma_1) \right]_{12} = 2i \lim_{\Lambda \to \infty} \Lambda \left[\sigma_3 \mathbf{A}(-\Lambda; X, T; \mathbf{c}) \sigma_3 \right]_{12}.$$

Now replacing Λ with $-\Lambda$ gives

$$(4.32) \qquad \Psi(-X, T; \mathbf{c}^* \sigma_1) = -2i \lim_{\Lambda \to \infty} \Lambda \left[\sigma_3 \mathbf{A}(\Lambda; X, T; \mathbf{c}) \sigma_3 \right]_{12} = \Psi(X, T; \mathbf{c}),$$

as desired. $\qquad \square$

Now we prove (1.19).

Lemma 4. $\Psi(X, -T; \mathbf{c})^* = \Psi(X, T; \mathbf{c})$ *if* $\mathbf{c} \in \mathbb{R}^2$. *In particular,* $\Psi(X, 0; \mathbf{c})$ *is real-valued when* $\mathbf{c} \in \mathbb{R}^2$.

Proof. Let $\mathbf{A}(\Lambda; X, T)$ be the unique solution of Riemann-Hilbert Problem 3 with given $\mathbf{c} \in \mathbb{R}^2$ and $(X, T) \in \mathbb{R}^2$. Note that $\mathbf{S} \in \mathbb{R}^{2 \times 2}$ and that the jump matrix $\mathbf{V_A}(\Lambda; X, T; \mathbf{c})$ defined in (4.25) admits the symmetry

$$
\begin{aligned}
\mathbf{V_A}(-\Lambda^*; X, -T; \mathbf{c})^* &= e^{-i(\Lambda X + \Lambda^2 T) \sigma_3} \mathbf{S}^* e^{-2i\Lambda^{-1} \sigma_3} (\mathbf{S}^*)^{-1} e^{i(\Lambda X + \Lambda^2 T) \sigma_3} \\
(4.33) \qquad &= e^{-i(\Lambda X + \Lambda^2 T) \sigma_3} \mathbf{S} e^{-2i\Lambda^{-1} \sigma_3} \mathbf{S}^{-1} e^{i(\Lambda X + \Lambda^2 T) \sigma_3} \\
&= \mathbf{V_A}(\Lambda; X, T; \mathbf{c}).
\end{aligned}
$$

Thus, the matrix function $\widehat{\mathbf{A}}(\Lambda; X, T; \mathbf{c}) := \mathbf{A}(-\Lambda^*; X, -T; \mathbf{c})^*$ satisfies the jump condition

$$(4.34) \qquad \widehat{\mathbf{A}}_+(\Lambda; X, T; \mathbf{c}) = \widehat{\mathbf{A}}_-(\Lambda; X, T; \mathbf{c}) \mathbf{V_A}(\Lambda; X, T; \mathbf{c}), \quad |\Lambda| = 1,$$

which is exactly the jump condition (4.3) in Riemann-Hilbert Problem 3. Moreover, $\widehat{\mathbf{A}}(\Lambda; X, T; \mathbf{c})$ is well-defined and analytic away from $|\Lambda| = 1$, $\det \widehat{\mathbf{A}}(\Lambda; X, T; \mathbf{c}) = 1$ on its domain of definition, and $\widehat{\mathbf{A}}(\Lambda; X, T; \mathbf{c}) \to \mathbb{I}$ as $\Lambda \to \infty$. Therefore, $\widehat{\mathbf{A}}(\Lambda; X, T; \mathbf{c}) = \mathbf{A}(-\Lambda^*; X, -T; \mathbf{c})^*$ also solves Riemann-Hilbert Problem 3. Uniqueness implies

$$(4.35) \qquad \mathbf{A}(\Lambda; X, T; \mathbf{c}) = \mathbf{A}(-\Lambda^*; X, -T; \mathbf{c})^*.$$

Using (4.35),

$$
\begin{aligned}
\Psi(X, -T) &= 2i \lim_{\Lambda \to \infty} \Lambda \left[\mathbf{A}(\Lambda; X, -T) \right]_{12} = 2i \lim_{\Lambda \to \infty} \Lambda \left[\mathbf{A}(-\Lambda^*; X, T)^* \right]_{12} \\
(4.36) \qquad &= - \left(2i \lim_{\Lambda \to \infty} \Lambda^* \left[\mathbf{A}(-\Lambda^*; X, T) \right]_{12} \right)^*.
\end{aligned}
$$

Now replacing Λ with $-\Lambda^*$ gives

$$(4.37) \qquad \Psi(X, -T) = \left(2i \lim_{\Lambda \to \infty} \Lambda \left[\mathbf{A}(\Lambda; X, T) \right]_{12} \right)^* = \Psi(X, T)^*,$$

which completes the proof. $\qquad \square$

Lemmas 1, 2, 3, and 4, combined with the fact that $\Psi(X, T; \mathbf{c})$ satisfies the second member of the Painlevé-III hierarchy given in (1.16), prove Theorem 2(b).

4.3. **The Painlevé-III function u(x): Proof of Theorem 2(c).** Inserting the definition (1.20) into the Painlevé-III equation (1.21) and using the chain rule to convert s-derivatives to X-derivatives shows that (1.21) is satisfied as long as

$$(4.38) \qquad X\Psi\Psi_{XXX} + 3\Psi\Psi_{XX} - X\Psi_X\Psi_{XX} - 2(\Psi_X)^2 + 4\Psi^4 + 2X\Psi^3\Psi_X + 2X\Psi^3\Psi_X = 0,$$

which holds from (1.16) since $T = 0$ and $\Psi(X, 0; \mathbf{c})$ is a real-valued function (since $\mathbf{c} \in \mathbb{R}^2$). Plugging the expansion $\Psi(X, 0; \mathbf{c}) = \Psi(0, 0; \mathbf{c}) + \Psi_X(0, 0; \mathbf{c})X + \mathcal{O}(X^2)$ as $X \to 0$ into the definition (1.20) along with $X = -\frac{1}{8}s^2$ immediately gives the expansion

$$(4.39) \qquad u(s; \mathbf{c}) = s + \frac{\Psi_X(0, 0; \mathbf{c})}{8\Psi(0, 0; \mathbf{c})}s^3 + \mathcal{O}(s^5), \quad x \to 0.$$

Using the explicit forms for $\Psi(0, 0; \mathbf{c})$ and $\Psi_X(0, 0; \mathbf{c})$ given in (1.17) shows (1.22). Higher derivatives $u^{(j)}(0; \mathbf{c})$, $j \geq 5$ can now be computed using the governing Painlevé-III equation (1.21). This completes the proof of Theorem 2.

APPENDIX A. REFORMULATION OF THE RIEMANN-HILBERT PROBLEM AS A LINEAR SYSTEM

We now show how to rewrite Riemann-Hilbert Problem 1 for $\mathbf{M}^{[n]}$ as the linear system (A.26) of $4n$ equations in $4n$ unknowns. In principal, this linear system can be solved explicitly for any fixed n, thus allowing the determination of $\psi^{[2n]}(x, t)$ via (A.17). In practice, the entries of the resulting coefficient matrix are increasingly complicated functions of x and t as n increases, and the system can only be feasibly solved for at most a few values of n. However, picking specific values of x and t reduces the problem to the inversion of a $4n \times 4n$ matrix with numerical entries, which can be done rapidly to any desired precision using standard numerical linear algebra packages for moderately large values of n. This procedure was used to create Figures 1–9. Analogous methods have been used previously to study semiclassical behavior of the nonlinear Schrödinger equation [20], the sine-Gordon equation [10], and the three-wave resonant interaction equations [9].

From (2.30) and (2.25) we have, using $\mathbf{M}^{[0]}(\lambda; x, t) \equiv \mathbb{I}$,

$$(A.1)$$
$$\mathbf{M}^{[n]}(\lambda; x, t) = \begin{cases} \mathbf{G}^{[n-1]}(\lambda; x, t) \cdots \mathbf{G}^{[0]}(\lambda; x, t), & \lambda \notin D_0, \\ \mathbf{G}^{[n-1]}(\lambda; x, t) \cdots \mathbf{G}^{[0]}(\lambda; x, t)e^{-i(\lambda x + \lambda^2 t)\sigma_3}\mathbf{G}^{[0]}(\lambda; 0, 0)^{-n}e^{i(\lambda x + \lambda^2 t)}, & \lambda \in D_0. \end{cases}$$

For succinctness we define

$$(A.2) \qquad \mathbf{\Pi}^{[n]}(\lambda; x, t) := \mathbf{G}^{[n-1]}(\lambda; x, t) \cdots \mathbf{G}^{[0]}(\lambda; x, t).$$

From the jump condition (2.31), we have $\mathbf{M}_-^{[n]}(\lambda; x, t) = \mathbf{M}_+^{[n]}(\lambda; x, t)\mathbf{V}_{\mathbf{M}}^{[n]}(\lambda; x, t)^{-1}$. Since the left-hand side extends analytically into D_0, the right-hand side must as well. Our conditions for the linear system will arise from the fact that

$$(A.3) \qquad \mathbf{M}_+^{[n]}(\lambda; x, t)\mathbf{V}_{\mathbf{M}}^{[n]}(\lambda; x, t)^{-1} = \mathbf{\Pi}^{[n]}(\lambda; x, t)e^{-i(\lambda x + \lambda^2 t)\sigma_3}\mathbf{G}^{[0]}(\lambda; 0, 0)^{-n}e^{i(\lambda x + \lambda^2 t)\sigma_3}$$

is analytic at ξ and ξ^*. We can write

$$(A.4) \qquad \mathbf{G}^{[0]}(\lambda; 0, 0)^{-1} = \mathbb{I} + \frac{\mathbf{W}}{\lambda - \xi} + \frac{\mathbf{X}}{\lambda - \xi^*},$$

where (recall $\xi = \alpha + i\beta$)

$$(A.5)$$
$$\mathbf{W} := \frac{2i\beta}{|\mathbf{c}|^2}\begin{pmatrix} c_1 c_1^* & c_1 c_2^* \\ c_1^* c_2 & c_2 c_2^* \end{pmatrix} = \frac{2i\beta}{|\mathbf{c}|^2}\begin{pmatrix} c_1 & c_1 \\ c_2 & c_2 \end{pmatrix}\begin{pmatrix} c_1^* & 0 \\ 0 & c_2^* \end{pmatrix},$$
$$\mathbf{X} := \frac{-2i\beta}{|\mathbf{c}|^2}\begin{pmatrix} c_2 c_2^* & -c_1 c_2^* \\ -c_1^* c_2 & c_1 c_1^* \end{pmatrix} = \frac{-2i\beta}{|\mathbf{c}|^2}\begin{pmatrix} c_2^* & c_2^* \\ -c_1^* & -c_1^* \end{pmatrix}\begin{pmatrix} c_2 & 0 \\ 0 & -c_1 \end{pmatrix}.$$

By direct calculation, we have the relations

$$(A.6) \qquad \mathbf{W}\mathbf{X} = \mathbf{X}\mathbf{W} = \mathbf{0}, \quad \mathbf{X}^2 = -2i\beta\mathbf{X}, \quad \mathbf{W}^2 = 2i\beta\mathbf{W}.$$

Using these, we have

$$(A.7) \qquad \begin{aligned} \mathbf{G}^{[0]}(\lambda; 0, 0)^{-n} &= \mathbb{I} + \sum_{k=1}^{n} \binom{n}{k} \left(\frac{\mathbf{W}^k}{(\lambda - \xi)^k} + \frac{\mathbf{X}^k}{(\lambda - \xi^*)^k} \right) \\ &= \mathbb{I} + \sum_{k=1}^{n} \binom{n}{k} (2i\beta)^{k-1} \left(\frac{\mathbf{W}}{(\lambda - \xi)^k} + (-1)^k \frac{\mathbf{X}}{(\lambda - \xi^*)^k} \right). \end{aligned}$$

Dropping the explicit dependence on n, we now set

$$(A.8) \qquad \mathbf{L}(\lambda; x, t) := \mathbf{\Pi}^{[n]}(\lambda; x, t) e^{-i(\lambda x + \lambda^2 t)\sigma_3}.$$

Therefore, the condition that the quantity in (A.3) is analytic at $\lambda = \xi$ and $\lambda = \xi^*$ can be reformulated as the fact that $\mathbf{L}(\lambda; x, t)\mathbf{G}^{[0]}(\lambda; 0, 0)^{-n}$ is analytic at $\lambda = \xi$ and $\lambda = \xi^*$. We expand $\mathbf{L}$ (which has poles of order n at ξ and ξ^*) about $\lambda = \xi$ and $\lambda = \xi^*$:

$$(A.9) \qquad \mathbf{L}(\lambda; x, t) = \sum_{j=-n}^{\infty} \mathbf{L}_j^+(x, t)(\lambda - \xi)^j, \quad \mathbf{L}(\lambda; x, t) = \sum_{j=-n}^{\infty} \mathbf{L}_j^-(x, t)(\lambda - \xi^*)^j.$$

Here the unknown 2×2 matrices $\mathbf{L}_j^{\pm}$ are independent of λ. Using the expansions (A.7) and (A.9), along with (A.6), the analyticity conditions become

$$(A.10)$$
$$\left(\sum_{j=-n}^{\infty} \mathbf{L}_j^+(\lambda - \xi)^j \right) \left(\mathbb{I} + \sum_{k=1}^{n} \binom{n}{k} (2i\beta)^{k-1} \left(\frac{\mathbf{W}}{(\lambda - \xi)^k} + (-1)^k \frac{\mathbf{X}}{(\lambda - \xi^*)^k} \right) \right) = \mathcal{O}(1), \quad \lambda \to \xi$$

and

$$(A.11)$$
$$\left(\sum_{j=-n}^{\infty} \mathbf{L}_j^-(\lambda - \xi^*)^j \right) \left(\mathbb{I} + \sum_{k=1}^{n} \binom{n}{k} (2i\beta)^{k-1} \left(\frac{\mathbf{W}}{(\lambda - \xi)^k} + (-1)^k \frac{\mathbf{X}}{(\lambda - \xi^*)^k} \right) \right) = \mathcal{O}(1), \quad \lambda \to \xi^*.$$

Expanding (A.10) and collecting powers of $\lambda - \xi$ gives $2n$ equations for $\mathbf{L}_{-n}^+, \dots, \mathbf{L}_{n-1}^+$. For example, for $n = 1$ we obtain the two equations

$$(A.12) \qquad \mathbf{L}_{-1}^+ \mathbf{W} = \mathbf{0}, \quad \mathbf{L}_{-1}^+ - \frac{1}{\xi - \xi^*} \mathbf{L}_{-1}^+ \mathbf{X} + \mathbf{L}_0^+ \mathbf{W} = \mathbf{0}.$$

Multiplying the second equation by $\mathbf{W}$ on the right and then using the first equation and the relations (A.6) yields the simplified equation $\mathbf{L}_0^+ \mathbf{W} = \mathbf{0}$. Indeed, using the same procedure of right-multiplying by $\mathbf{W}$ and using forward substitution and (A.6) works for general n to deliver the equations $\mathbf{L}_j^+ \mathbf{W} = \mathbf{0}$, $-n \le j \le n-1$. Similarly, expanding (A.11) and collecting powers of $\lambda - \xi^*$ gives, after analogous manipulations, the equations $\mathbf{L}_j^- \mathbf{X} = \mathbf{0}$, $-n \le j \le n-1$. From the explicit forms (A.5) for $\mathbf{W}$ and $\mathbf{X}$, we see these matrix equations are equivalent to the vector equations

$$(A.13) \qquad \mathbf{L}_j^+ \begin{pmatrix} c_1 \\ c_2 \end{pmatrix} = \mathbf{0}, \quad \mathbf{L}_j^- \begin{pmatrix} c_2^* \\ -c_1^* \end{pmatrix} = \mathbf{0}, \quad -n \le j \le n-1.$$

Next, recalling $\mathbf{L} = \mathbf{\Pi}^{[n]} e^{-i(\lambda x + \lambda^2 t)\sigma_3}$, we expand

$$(A.14) \qquad e^{-i(\lambda x + \lambda^2 t)\sigma_3} = \sum_{j=0}^{\infty} \mathbf{D}_j^+(x, t)(\lambda - \xi)^j = \sum_{j=0}^{\infty} \mathbf{D}_j^-(x, t)(\lambda - \xi^*)^j$$

(here the coefficient matrices $\mathbf{D}_j^{\pm}$ are known, or at least can be computed) and

(A.15) $$\boldsymbol{\Pi}^{[n]}(\lambda; x, t) = \mathbb{I} + \sum_{j=1}^{n} \left(\frac{\mathbf{A}_{-j}^{+}(x,t)}{(\lambda - \xi)^j} + \frac{\mathbf{A}_{-j}^{-}(x,t)}{(\lambda - \xi^*)^j} \right)$$

(here the coefficient matrices $\mathbf{A}_{-j}^{\pm}$ are unknown). If we write

(A.16) $$\mathbf{A}_{-j}^{+} =: \begin{pmatrix} r_{-j} & u_{-j} \\ * & * \end{pmatrix}, \quad \mathbf{A}_{-j}^{-} =: \begin{pmatrix} s_{-j} & v_{-j} \\ * & * \end{pmatrix},$$

(here * denotes an entry we will not need), then

(A.17) $$\psi^{[2n]}(x, t) = 2i(u_{-1}(x, t) + v_{-1}(x, t)).$$

Since the equations for the entries in the top and bottom rows in (A.13) decouple, we only need to calculate the first rows of the matrices $\mathbf{A}_{-j}^{\pm}$ to reconstruct $\psi^{[2n]}(x, t)$. This gives $4n$ linear equations in $4n$ unknowns, which we now express in a form suitable for numerical computations.

Direct calculation gives

(A.18) $$\mathbf{L}_j^{+} = \sum_{k=0}^{j+n} \mathbf{A}_{j-k}^{+} \mathbf{D}_k^{+}, \quad \mathbf{L}_j^{-} = \sum_{k=0}^{j+n} \mathbf{A}_{j-k}^{-} \mathbf{D}_k^{-}, \quad -n \leq j \leq -1.$$

Furthermore, if we define the constants $\gamma_{k,m}^{\pm}$ by the expansions

(A.19) $$\frac{1}{(\lambda - \xi^*)^m} = \sum_{k=0}^{\infty} \gamma_{k,m}^{+} (\lambda - \xi)^k, \quad \frac{1}{(\lambda - \xi)^m} = \sum_{k=0}^{\infty} \gamma_{k,m}^{-} (\lambda - \xi^*)^k,$$

then we also have

(A.20) $$\begin{aligned} \mathbf{L}_j^{+} &= \mathbf{D}_j^{+} + \sum_{k=1}^{n} \mathbf{A}_{-k}^{+} \mathbf{D}_{j+k}^{+} + \sum_{\ell=0}^{j} \left(\sum_{m=1}^{n} \gamma_{j-\ell,m}^{+} \mathbf{A}_{-m}^{-} \right) \mathbf{D}_{\ell}^{+}, \\ \mathbf{L}_j^{-} &= \mathbf{D}_j^{-} + \sum_{k=1}^{n} \mathbf{A}_{-k}^{-} \mathbf{D}_{j+k}^{-} + \sum_{\ell=0}^{j} \left(\sum_{m=1}^{n} \gamma_{j-\ell,m}^{-} \mathbf{A}_{-m}^{+} \right) \mathbf{D}_{\ell}^{-}, \end{aligned} \quad 0 \leq j \leq n-1.$$

Comparing (A.13) with (A.18) and (A.20), we see that $\mathbf{D}_j^{+}$ only occurs multiplied by $(c_1, c_2)^{\mathsf{T}}$, and $\mathbf{D}_j^{-}$ only occurs multiplied by $(c_2^*, -c_1^*)^{\mathsf{T}}$, so we define

(A.21) $$\begin{pmatrix} f_j^{+}(x, t) \\ g_j^{+}(x, t) \end{pmatrix} := \mathbf{D}_j^{+}(x, t) \begin{pmatrix} c_1 \\ c_2 \end{pmatrix}, \quad \begin{pmatrix} f_j^{-}(x, t) \\ g_j^{-}(x, t) \end{pmatrix} := \mathbf{D}_j^{-}(x, t) \begin{pmatrix} c_2^* \\ -c_1^* \end{pmatrix}, \quad 0 \leq j \leq 2n-1.$$

We also define

$$\mathbf{F}_j := \begin{pmatrix} f_j^{+} & 0 \\ 0 & f_j^{-} \end{pmatrix}, \quad \mathbf{G}_j := \begin{pmatrix} g_j^{+} & 0 \\ 0 & g_j^{-} \end{pmatrix},$$

(A.22) $$\mathbf{H}_{jk} := \begin{pmatrix} 0 & \sum_{\ell=0}^{j} \gamma_{\ell k}^{+} f_{j-\ell}^{+} \\ \sum_{\ell=0}^{j} \gamma_{\ell k}^{-} f_{j-\ell}^{-} & 0 \end{pmatrix}, \quad \mathbf{I}_{jk} := \begin{pmatrix} 0 & \sum_{\ell=0}^{j} \gamma_{\ell k}^{+} g_{j-\ell}^{+} \\ \sum_{\ell=0}^{j} \gamma_{\ell k}^{-} g_{j-\ell}^{-} & 0 \end{pmatrix}.$$

Using these, we define the $4n \times 4n$ coefficient matrix

(A.23)
$$
\mathbf{T} := \begin{pmatrix}
\mathbf{F}_0 & \mathbf{G}_0 & \mathbf{0} & \mathbf{0} & \cdots & \mathbf{0} & \mathbf{0} \\
\mathbf{F}_1 & \mathbf{G}_1 & \mathbf{F}_0 & \mathbf{G}_0 & \cdots & \mathbf{0} & \mathbf{0} \\
\vdots & \vdots & \vdots & \vdots & & \vdots & \vdots \\
\mathbf{F}_{n-1} & \mathbf{G}_{n-1} & \mathbf{F}_{n-2} & \mathbf{G}_{n-2} & \cdots & \mathbf{F}_0 & \mathbf{G}_0 \\
\mathbf{F}_n + \mathbf{H}_{0,n} & \mathbf{G}_n + \mathbf{I}_{0,n} & \mathbf{F}_{n-1} + \mathbf{H}_{0,n-1} & \mathbf{G}_{n-1} + \mathbf{I}_{0,n-1} & \cdots & \mathbf{F}_1 + \mathbf{H}_{0,1} & \mathbf{G}_1 + \mathbf{I}_{0,1} \\
\mathbf{F}_{n+1} + \mathbf{H}_{1,n} & \mathbf{G}_{n+1} + \mathbf{I}_{1,n} & \mathbf{F}_n + \mathbf{H}_{1,n-1} & \mathbf{G}_n + \mathbf{I}_{1,n-1} & \cdots & \mathbf{F}_2 + \mathbf{H}_{1,1} & \mathbf{G}_2 + \mathbf{I}_{1,1} \\
\vdots & \vdots & \vdots & \vdots & & \vdots & \vdots \\
\mathbf{F}_{2n-1} + \mathbf{H}_{n-1,n} & \mathbf{G}_{2n-1} + \mathbf{I}_{n-1,n} & \mathbf{F}_{2n-2} + \mathbf{H}_{n-1,n-1} & \mathbf{G}_{2n-2} + \mathbf{I}_{n-1,n-1} & \cdots & \mathbf{F}_n + \mathbf{H}_{n-1,1} & \mathbf{G}_n + \mathbf{I}_{n-1,1}
\end{pmatrix},
$$

the $4n$-vector of unknowns

(A.24)
$$
\mathbf{y} := \begin{pmatrix} r_{-n} & s_{-n} & u_{-n} & v_{-n} & \cdots & r_{-1} & s_{-1} & u_{-1} & v_{-1} \end{pmatrix},
$$

and the $4n$-vector of inhomogeneous terms

(A.25)
$$
\mathbf{f} := (\underbrace{0 \; 0 \; \cdots \; 0}_{2n \text{ terms}} \; -f_0^+ \; -f_0^- \; -f_1^+ \; -f_1^- \; \cdots \; -f_{n-1}^+ \; -f_{n-1}^-).
$$

Here $\mathbf{T}$, $\mathbf{y}$, and $\mathbf{f}$ depend on x, t, n, $\mathbf{c}$, and ξ. At last, the equations for the top rows in (A.13) can be recast as

(A.26)
$$
\mathbf{T}\mathbf{y} = \mathbf{f},
$$

a form amenable to numerical computation for moderately large values of n. Once $\mathbf{y}$ is obtained from solving this equation, the solution $\psi^{[2n]}(x,t)$ to the nonlinear Schrödinger equation is immediately recovered from (A.17).

APPENDIX B. NUMERICAL COMPUTATION OF $\Psi(X,T;\mathbf{c})$ FOR ARBITRARY $\mathbf{c} \in (\mathbb{C}^*)^2$

A numerical procedure was developed in [7, §5] to compute the special functions $\Psi(X,T;(1,\pm1))$ for the first time, with the aid of RHPackage [24] in context of the numerical framework introduced in [31]. While Riemann-Hilbert Problem 3 can be solved numerically using RHPackage without contour deformations for (X,T) lying in a small rectangle containing the origin, e.g. $|X| + |T| < 2$, for large values of X one needs to deform the jump contours of this Riemann-Hilbert Problem by introducing lens-shaped domains to use the Deift-Zhou method of nonlinear steepest descent. In this section we briefly describe the deformations necessary to compute $\Psi(X,0;\mathbf{c})$ for arbitrary $\mathbf{c} \in (\mathbb{C}^*)^2$ and large values of X. These deformations are a generalization of what was employed in [7, §4.1] to arbitrary $\mathbf{c} \in (\mathbb{C}^*)^2$. Before we begin, we note it is sufficient to consider the case $X \geq 0$ by (1.18) and $T \geq 0$ by (1.19).

The function $\mathbf{B}(\Lambda; X,T)$ defined in (4.12) is unimodular and satisfies the following Riemann-Hilbert problem.

Riemann-Hilbert Problem 4 (Reformulated near-field problem)**.** *Let $(X,T) \in \mathbb{R}^2$ be fixed but arbitrary parameters. Find the unique 2×2 matrix-valued function $\mathbf{B}(\Lambda; X,T)$ with the following properties:*

*   ***Analyticity:*** *$\mathbf{B}(\Lambda; X,T)$ is analytic for $|\Lambda| \neq 1$ and takes continuous boundary values from the interior and exterior of the jump contour.*
*   ***Jump condition:*** *The boundary values on the jump contour (oriented clockwise) follow the relation*

(B.1)
$$
\mathbf{B}_+(\Lambda; X,T) = \mathbf{B}_-(\Lambda; X,T) e^{-i(\Lambda X + \Lambda^2 T + 2\Lambda^{-1})\sigma_3} \mathbf{S}^{-1} e^{i(\Lambda X + \Lambda^2 T + 2\Lambda^{-1})\sigma_3}, \quad |\Lambda| = 1.
$$

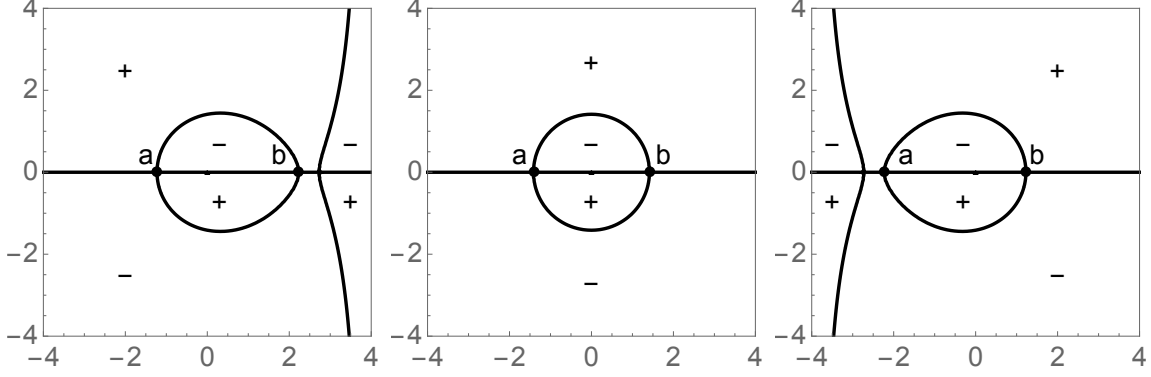*   ***Normalization:*** *$\mathbf{B}(\Lambda; X,T) \to \mathbb{I}$ as $\Lambda \to \infty$.*

FIGURE 12. Signature charts of $\Im(\phi(z;v))$ in the complex z-plane. *Left:* $v = -0.134$ (representative for $-54^{-1/2} < v < 0$). *Center:* $v = 0$. *Right:* $v = 0.134$ (representative for $0 < v < 54^{-1/2}$).

To solve Riemann-Hilbert Problem 4 for $X > 0$ large, we introduce

(B.2) $$v := X^{-3/2}T, \quad z := X^{1/2}\Lambda$$

and define $\mathbf{C}(z; X, v) := \mathbf{B}(X^{-1/2}z; X, X^{3/2}v)$. Recall that $\Psi(X, T; \mathbf{c})$ is recovered from $\mathbf{B}(\Lambda; X, T)$ via (4.15), which implies

(B.3) $$\Psi(X, X^{3/2}v) = 2iX^{-1/2} \lim_{z \to \infty} z\,[\mathbf{C}(z; X, v)]_{12}, \quad X > 0,$$

and the phase in the diagonal matrices conjugating $\mathbf{S}^{-1}$ in the jump condition (B.1) now has the form

(B.4) $$\Lambda X + \Lambda^2 T + 2\Lambda^{-1} = X^{1/2}(z + vz^2 + 2z^{-1}) =: X^{1/2}\phi(z; v).$$

It is clear that for each $X > 0$ and $v \geq 0$, $\mathbf{C}(z; X, v)$ satisfies the jump condition

(B.5) $$\mathbf{C}_+(z; X, v) = \mathbf{C}_-(z; X, v)e^{-iX^{1/2}\phi(z;v)\sigma_3}\mathbf{S}^{-1}e^{iX^{1/2}\phi(z;v)\sigma_3}, \quad z \in \Gamma,$$

where Γ is a Jordan curve (depending on X) surrounding $z = 0$ with clockwise orientation, and $\mathbf{C}(z; X, v)$ is analytic in the complement of Γ. The matrix $\mathbf{C}(z; X, v)$ is unimodular and has the same normalization as $\mathbf{B}(\Lambda; X, T)$: $\mathbf{C}(z; X, v) \to \mathbb{I}$ as $z \to \infty$ for each fixed $X > 0$ and $v \geq 0$.

We now proceed with introducing lens-shaped regions and deforming the jump contour to control the exponential factors in the jump matrix (B.5) as in [7]. For given $v \geq 0$, the critical points of the phase $\phi(z; v)$ are roots of the real cubic equation

(B.6) $$2vz^3 + z^2 - 2 = 0,$$

which are all real and distinct if $0 \leq v < 54^{-1/2}$. If $v > 54^{-1/2}$, however, there is a complex conjugate pair of roots and a real root. In the former case, the level curve $\Im(\phi(z; v)) = 0$ along which the exponential factors $e^{\pm iX^{1/2}\phi(z;v)\sigma_3}$ are purely oscillatory has a component that is a Jordan curve enclosing the origin in the z-plane, and that passes through two critical points, with the remaining critical point (if $v > 0$) in the exterior domain. We take this curve as the jump contour Γ in (B.5) for $\mathbf{C}(z; X, v)$ and denote the relevant two critical points of $\phi(z; v)$ by $a < b$, where a and b depend on v. Note that when $v = 0$, (B.6) is a real quadratic with the roots $a = -\sqrt{2}$ and $b = \sqrt{2}$. See Figure 12 for representative level curves $\Im(\phi(z; v)) = 0$ and the roots of (B.6) for different values of $v \in \mathbb{R}$.

The real axis splits Γ into two arcs, Γ^+ lying in the upper half plane and Γ^- lying in the lower half plane. We deform $\Gamma^\pm$ by opening lens-shaped domains $L^\pm$ and $R^\pm$ on the left and right sides of $\Gamma^\pm$. The outer boundary arcs $C_L^\pm$ and $C_R^\pm$ of these regions meet the real axis at $45°$ angles as

shown in the left-hand panel of Figure 13 and on each of these arcs $\Im(\phi(z;v))$ has a definite sign. The line segment from a to b is denoted I. We label the region between C_R^+ and the real axis by Ω^+, the region between C_R^- and the real axis by Ω^-, the region between $C_R^\pm$ and $\Gamma^\pm$ by $R^\pm$, and the region between $C_L^\pm$ and $\Gamma^\pm$ by $L^\pm$. See Figure 13 for illustrations of these domains and contour arcs.

To separate the exponential factors $e^{\pm iX^{1/2}\phi(z;v)}$ in the jump condition (B.5), we make the following substitutions:

$$(B.7) \qquad \mathbf{E}(z;X,v) := \begin{cases} \mathbf{C}(z;X,v)\begin{bmatrix} 1 & 0 \\ \frac{c_2}{c_1}e^{2iX^{1/2}\phi(z;v)} & 1 \end{bmatrix}, & z \in L^+, \\[2ex] \mathbf{C}(z;X,v)\left(\frac{|\mathbf{c}|}{c_1}\right)^{\sigma_3}\begin{bmatrix} 1 & \frac{c_1 c_2^*}{|\mathbf{c}|^2}e^{-2iX^{1/2}\phi(z;v)} \\ 0 & 1 \end{bmatrix}, & z \in R^+, \\[2ex] \mathbf{C}(z;X,v)\left(\frac{|\mathbf{c}|}{c_1}\right)^{\sigma_3}, & z \in \Omega^+, \\[2ex] \mathbf{C}(z;X,v)\left(\frac{|\mathbf{c}|}{c_1^*}\right)^{-\sigma_3}, & z \in \Omega^-, \\[2ex] \mathbf{C}(z;X,v)\left(\frac{|\mathbf{c}|}{c_1^*}\right)^{-\sigma_3}\begin{bmatrix} 1 & 0 \\ -\frac{c_2 c_1^*}{|\mathbf{c}|^2}e^{2iX^{1/2}\phi(z;v)} & 1 \end{bmatrix}, & z \in R^-, \\[2ex] \mathbf{C}(z;X,v)\begin{bmatrix} 1 & -\frac{c_2^*}{c_1^*}e^{-2iX^{1/2}\phi(z;v)} \\ 0 & 1 \end{bmatrix}, & z \in L^-, \\[2ex] \mathbf{C}(z;X,v), & \text{otherwise.} \end{cases}$$

Now $\mathbf{C}_+(z;X,v) = \mathbf{C}_-(z;X,v)$ for $z \in \Gamma^\pm$, so this transformation removes the jump condition across Γ^+ and Γ^- and $\mathbf{C}(z;X,v)$ can be considered to be a well-defined analytic function on Γ^+ and Γ^-. Moreover, $\mathbf{C}(z;X,v)$ is unimodular and has the normalization $\lim_{z\to\infty}\mathbf{C}(z;X,v) = \mathbb{I}$. It therefore is the solution of the following Riemann-Hilbert problem.

Riemann-Hilbert Problem 5 (Large-X problem)**.** *Let $(X,v) \in \mathbb{R}_{>0} \times \mathbb{R}_{\geq 0}$ be fixed but arbitrary parameters. Find the unique 2×2 matrix-valued function $\mathbf{E}(z;X,v)$ with the following properties:*

Analyticity: *$\mathbf{E}(z;X,v)$ is analytic in z for $z \in \mathbb{C} \setminus (C_L^- \cup C_R^- \cup I \cup C_R^+ \cup C_L^+)$, and it takes continuous boundary values from the interior and exterior of the union of the five arcs $C_L^- \cup C_R^- \cup I \cup C_R^+ \cup C_L^+$.*

Jump condition: *The boundary values on the jump contour $C_L^- \cup C_R^- \cup I \cup C_R^+ \cup C_L^+$ follow the relations*

$$(B.8) \qquad \mathbf{E}_+(z;X,v) = \mathbf{E}_-(z;X,v)\begin{bmatrix} 1 & 0 \\ -\frac{c_2}{c_1}e^{2iX^{1/2}\phi(z;v)} & 1 \end{bmatrix}, \quad z \in C_L^+,$$

$$(B.9) \qquad \mathbf{E}_+(z;X,v) = \mathbf{E}_-(z;X,v)\begin{bmatrix} 1 & \frac{c_1 c_2^*}{|\mathbf{c}|^2}e^{-2iX^{1/2}\phi(z;v)} \\ 0 & 1 \end{bmatrix}, \quad z \in C_R^+,$$

$$(B.10) \qquad \mathbf{E}_+(z;X,v) = \mathbf{E}_-(z;X,v)\left(\frac{|\mathbf{c}|^2}{|c_1|^2}\right)^{\sigma_3}, \quad z \in I,$$

$$(B.11) \qquad \mathbf{E}_+(z;X,v) = \mathbf{E}_-(z;X,v)\begin{bmatrix} 1 & 0 \\ -\frac{c_2 c_1^*}{|\mathbf{c}|^2}e^{2iX^{1/2}\phi(z;v)} & 1 \end{bmatrix}, \quad z \in C_R^-,$$

$$(B.12) \qquad \mathbf{E}_+(z;X,v) = \mathbf{E}_-(z;X,v)\begin{bmatrix} 1 & -\frac{c_2^*}{c_1^*}e^{-2iX^{1/2}\phi(z;v)} \\ 0 & 1 \end{bmatrix}, \quad z \in C_L^-.$$

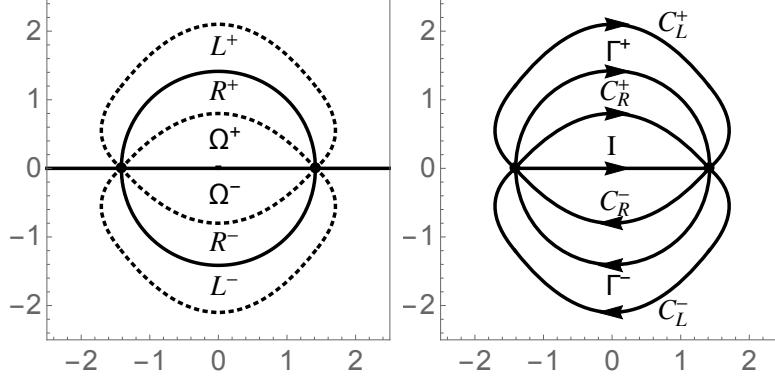**Normalization:** *$\mathbf{E}(z;X,v) \to \mathbb{I}$ as $z \to \infty$.*

FIGURE 13. *Left:* The regions $\Omega^\pm$, $R^\pm$, and $L^\pm$ used in the definition of $\mathbf{E}(z; X, v)$. *Right:* The jump contours for Riemann-Hilbert Problem 5. In both plots $v = 0$.

Since $\Im(\phi(z; v)) > 0$ for $z \in C_L^+ \cup C_R^-$ and $\Im(\phi(z; v)) < 0$ for $z \in C_R^+ \cup C_L^-$, the jump matrices supported on these four contour arcs are exponentially small (as $X \to +\infty$) perturbations of the identity matrix uniformly except near the end points a and b. For the jump contours in Riemann-Hilbert Problem 5 with $v = 0$, see the right panel of Figure 13. The picture is completely analogous for $0 < v < 54^{-1/2}$.

Riemann-Hilbert Problem 5 can be used to numerically compute $\Psi(X, T)$ for values of $X > 54^{1/3}T^{2/3}$. We now focus our attention on the case $T = 0$ (hence $v = 0$) and $\mathbf{c} \in \mathbb{R}^2$. For cross-validation of the numerical procedure described here along with further details, see [7, §5].

As discussed in [7, §5], although the jump matrices on the four arcs $C_L^- \cup C_R^- \cup C_R^+ \cup C_L^+$ become exponentially small perturbations of the identity matrix as $X \to \infty$, their Sobolev norms (differentiation with respect to z) grow. This presents a numerical challenge that is overcome in RHPackage by a rescaling algorithm (see [31] for details). Thus, to have a procedure that is asymptotically robust as $X > 0$ becomes large, one has to remove the so-called connecting jump condition (B.10) on the line segment I. To this end, we introduce the parametrix

$$(B.13) \qquad \mathbf{\Delta}(z; v) := \left(\frac{z - a(v)}{z - b(v)} \right)^{ip\sigma_3}, \quad p := \frac{\ln\left(\frac{|\mathbf{c}|^2}{|c_1|^2} \right)}{2\pi} > 0, \quad z \in \mathbb{C} \setminus I,$$

which exactly satisfies the jump condition

$$(B.14) \qquad \mathbf{\Delta}_+(z; v) = \mathbf{\Delta}_-(z; v) \left(\frac{|\mathbf{c}|^2}{|c_1|^2} \right)^{\sigma_3}, \quad z \in I,$$

and is normalized as $\mathbf{\Delta}(z; v) \to \mathbb{I}$ as $z \to \infty$. Thus, setting $\widehat{\mathbf{C}}(z; X, v) := \mathbf{C}(z; X, v)\mathbf{\Delta}(z; v)^{-1}$ for $z \in \mathbb{C} \backslash I$ removes the connecting jump condition across I as desired and conjugates the existing other jump matrices given in (B.8)–(B.12) by $\mathbf{\Delta}(z; v)$. This comes with the cost of introducing bounded singularities in the jump matrices at $z = a$ and $z = b$ since $\mathbf{\Delta}(z; v)$ has bounded singularities at these points. To remedy this, we place small circles centered at $z = a$ and $z = b$ and transfer the jump conditions on the line segments inside these circles to jump conditions on arcs of these circles connecting the endpoints of these line segments. This successfully removes the aforementioned singular jump conditions, but introduces jump matrices on the small circles centered at $z = a(v)$ and $z = b(v)$ whose components now grow exponentially as $X \to +\infty$. Observe that for $p = a, b$,

$$(B.15) \qquad \phi(z; v) - \phi(p; v) = \frac{\phi''(p; v)}{2}(z - p)^2 + \mathcal{O}((z - p)^3), \quad z \to p.$$

Therefore,

$$e^{\pm i|X|^{1/2}\phi(z;v)} = \mathcal{O}(1), \quad X \to +\infty \tag{B.16}$$

if $|z-p| = \mathcal{O}(|X|^{-1/4})$ as $X \to +\infty$ for both $p = a(v)$ and $p = b(v)$. In order to overcome the growth of these factors, we scale the common radius of these circles by $|X|^{-1/4}$ as X becomes large. As noted in [7, §5], while shrinking the circles at a faster rate ensures boundedness of the exponentials supported on them, it also moves the support of the jump matrices closer to singularities at a faster rate and hence should be avoided. The jump contours of the Riemann-Hilbert problem used to compute $\Psi(X,0)$ numerically for large values of $X > 0$ are given in Figure 14. In practice, the jump contours are truncated if the jump matrices supported on them differ from the identity matrix by at most machine precision. For more details see [31, Chapter 2 and Chapter 7] and [7, §5].
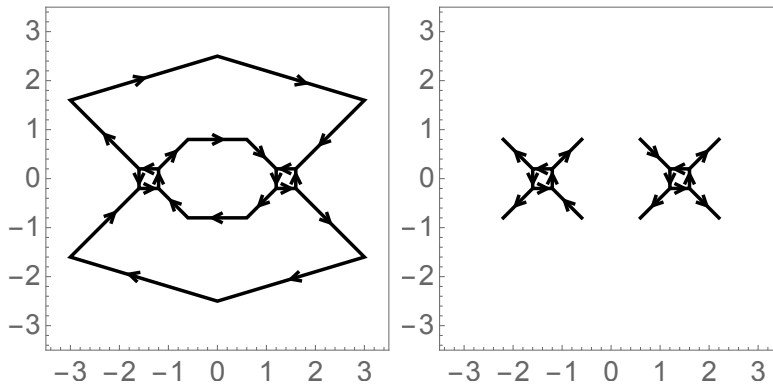

FIGURE 14. *Left:* Jump contours used in the numerical solution of the Riemann-Hilbert problem satisfied by $\widehat{\mathbf{C}}(z; X, v = 0)$, which is asymptotically and numerically well-adapted for large $X > 0$. *Right:* Truncated jump contours that are used in practice if $X > 0$ is large. For both plots, $X = 2000$ and $v = 0$.

References

[1] M. Ablowitz, S. Chakravarty, A. Trubatch, and J. Villarroel, A novel class of solutions of the non-stationary Schrödinger and the Kadomtsev-Petviashvili I equations, *Phys. Lett. A* **267**, 132–146 (2000).

[2] T. Aktosun, F. Demontis, and C. van der Mee, Exact solutions to the focusing nonlinear Schrödinger equation, *Inverse Problems* **23**, 2171–2195 (2007).

[3] T. Aktosun, F. Demontis, and C. van der Mee, Exact solutions to the sine-Gordon equation, *J. Math. Phys.* **51**, 123521 (2010).

[4] R. Beals and R. Coifman, Scattering and inverse scattering for first order systems, *Comm. Pure Appl. Math.* **37**, 39–90 (1984).

[5] D. Benney and A. Newell, The propagation of nonlinear wave envelopes, *J. Math. and Phys.* **46**, 133–139 (1967).

[6] M. Bertola and A. Tovbis, Universality for the focusing nonlinear Schrödinger equation at the gradient catastrophe point: rational breathers and poles of the tritronquée solution to Painlevé I, *Comm. Pure Appl. Math.* **66**, 678–752 (2013).

[7] D. Bilman, L. Ling, and P. Miller, Extreme superposition: rogue waves of infinite order and the Painlevé-III hierarchy, arXiv:1806.00545 (2018).

[8] D. Bilman and P. Miller, A robust inverse scattering transform for the focusing nonlinear Schrödinger equation, arXiv:1710.06568 (2017). To appear in *Comm. Pure Appl. Math.*

[9] R. Buckingham, R. Jenkins, and P. Miller, Semiclassical soliton ensembles for the three-wave resonant interaction equations, *Comm. Math. Phys.* **354**, 1015–1100 (2017).

[10] R. Buckingham and P. Miller, Exact solutions of semiclassical non-characteristic Cauchy problems for the sine-Gordon equation, *Physica D* **237**, 2296–2341 (2008).

[11] R. Buckingham and P. Miller, Large-degree asymptotics of rational Painlevé-II functions: noncritial behaviour, *Nonlinearity* **27**, 2489–2577 (2014).

[12] R. Chiao, E. Garmire, and C. Townes, Self-trapping of optical beams, *Phys. Rev. Lett.* **13**, 479–482 (1964).

[13] P. Deift and X. Zhou, A steepest descent method for oscillatory Riemann-Hilbert problems. Asymptotics for the MKdV equation, *Ann. of Math. (2)* **137**, 295–368 (1993).

[14] G. El and M. Hoefer, Dispersive shock waves and modulation theory, *Physica D* **333**, 11–65 (2016).

[15] B. Fuchssteiner and R. Aiyer, Multisolitons, or the discrete eigenfunctions of the recursion operator of non-linear evolution equations: II. Background, *J. Phys. A* **20**, 375–388 (1987).

[16] L. Gagnon and N. Stiévenart, N-soliton interaction in optical fibers: the multiple-pole case, *Opt. Lett.* **19**, 619–621 (1994).

[17] S. Kamvissis, K. McLaughlin, and P. Miller, *Semiclassical soliton ensembles for the focusing nonlinear Schrödinger equation*, Annals of Mathematics Studies **154**, Princeton University Press, Princeton, NJ, 2003.

[18] Y. Kuang and J. Zhu, The higher-order soliton solutions for the coupled Sasa-Satsuma system via the $\bar{\partial}$-dressing method, *Appl. Math. Lett.* **66**, 47–53 (2017).

[19] L. Ling, B. Feng, and Z. Zhu, Multi-soliton, multi-breather and higher order rogue wave solutions to the complex short pulse equation, *Phys. D* **327**, 13–29, (2016).

[20] G. Lyng and P. Miller, The N-soliton of the focusing nonlinear Schrödinger equation for N large, *Comm. Pure Appl. Math.* **60**, 951–1026 (2007).

[21] T. Martines, Generalized inverse scattering transform for the nonlinear Schrödinger equation for bound states with higher multiplicities, *Electron. J. Differential Equations* **179**, 1–15 (2017).

[22] V. Matveev and M. Salle, *Darboux transformations and solitons*, Springer-Verlag, Berlin, 1991.

[23] E. Olmedilla, Multiple pole solutions of the non-linear Schrödinger equation, *Physica D* **25**, 330–346 (1987).

[24] S. Olver, RHPackage, http://www.maths.usyd.edu.au/u/olver/projects/RHPackage.html, 2011.

[25] C. Pöppe, Construction of solutions of the sine-Gordon equation by means of Fredholm determinants, *Physica D* **9**, 103–139 (1983).

[26] A. Sakka, Linear problems and hierarchies of Painlevé equations, *J. Phys. A* **42**, 025210 (2009).

[27] C. Schiebold, Asymptotics for the multiple pole solutions of the nonlinear Schrödinger equation, *Nonlinearity* **30**, 2930–2981 (2017).

[28] V. Shchesnovich and J. Yang, Higher-order solitons in the N-wave system, *Stud. Appl. Math.* **110**, 297–332 (2003).

[29] B. Suleimanov, Effect of a small dispersion on self-focusing in a spatially one-dimensional case, *JETP Lett.* **106**, 400–405 (2017).

[30] S. Tanaka, Non-linear Schrödinger equation and modified Korteweg-de Vries equation; construction of solutions in terms of scattering data, *Publ. RIMS, Kyoto Univ.* **10**, 329–357 (1975).

[31] T. Trogdon and S. Olver, *Riemann-Hilbert problems, their numerical solution, and the computation of nonlinear special functions*, SIAM, Philadelphia, 2016.

[32] H. Tsuru and M. Wadati, The multiple pole solutions of the sine-Gordon equation, *J. Phys. Soc. Jpn.* **53**, 2908–2921 (1984).

[33] J. Villarroel and M. Ablowitz, On the discrete spectrum of the nonstationary Schrödinger equation and multipole lumps of the Kadomtsev-Petviashvili I equation, *Comm. Math. Phys.* **207**, 1–42 (1999).

[34] N. Vinh, Strongly interacting multi-solitons with logarithmic relative distance for the gKdV equation, *Nonlinearity* **30**, 4614–4648 (2017).

[35] M. Wadati and K. Ohkuma, Multiple-pole solutions of the modified Korteweg-de Vries equation, *J. Phys. Soc. Jpn.* **51**, 2029–2035 (1982).

[36] V. Zakharov, Stability of periodic waves of finite amplitude on the surface of a deep fluid, *J. Applied Mech. Tech. Phys.* **9**, 190–194 (1968).

[37] V. Zakharov and A. Shabat, Exact theory of two-dimensional self-focusing and one-dimensional self-modulation of waves in nonlinear media, *Soviet Physics JETP* **34**, 62–69 (1972). Translated from *Z. Eksper. Teoret. Fiz.* **61**, 118–134 (1971).